

Cyclic and Spirocyclic Polyacetal Ethers from Lignin-Based Aromatics

Alexander G. Pemba, Mayra Rostagno, Tanner A. Lee and Stephen A. Miller*

The George and Josephine Butler Polymer Research Laboratory, Department of Chemistry, University of Florida
Gainesville, Florida 32611-7200, USA

Electronic Supplementary Information (ESI)

Supplementary Information Available: Complete polymer characterization data.

Table of Contents

Summary of Polymerization Data	S2
Gel Permeation Chromatography (GPC) Analysis	S3
Differential Scanning Calorimetry (DSC) Thermograms	S10
Thermogravimetric Analysis (TGA) Thermograms	S14
^1H NMR Spectra	S18
^{13}C NMR Spectra	S22
Fourier Transform Infrared Spectroscopy (FTIR) Spectra	S26
Degradation Studies via Dynamic Light Scattering (DLS)	S28



Summary of Polymerization Data

Table S1. Thermal and molecular weight data for spirocyclic (1–4) and cyclic (5–8) polyacetal ethers.^a

Entry	Polymer	Yield (%)	M_w (Da)	M_n (Da)	PDI	T_g (°C)	T_m (°C)	T_{95} (°C) ^d	Residue (%) ^d
1 ^b P-BB		81	^c	^c	^c	n.o.	n.o.	328	20
2 P-VV		90	23,700	10,600	2.2	129	n.o.	308	19
3 P-SS		90	36,000	18,600	1.9	152	n.o.	307	17
4 P-EE		83	47,800	18,500	2.6	108	n.o.	326	23
5 D-BB		81	3,500	2,600 ^e	1.4	n.o.	259	349	8.3
6 D-VV		90	44,200	22,200	2.0	80	n.o.	327	8.2
7 D-SS		90	34,600	21,600	1.6	98	n.o.	320	12
8 D-EE		83	42,100	19,300	2.2	68	n.o.	333	10

^aPolymerization conducted in refluxing methylene chloride at 40 °C, except as noted. Molecular weight data obtained by GPC in hexafluoroisopropanol (HFIP) solvent. For DSC data, n.o. indicates a thermal transition not observed. ^bPolymerization conducted in refluxing 1,1,2,2-tetrachloroethane at 146 °C. ^cAlthough insolubility prevented GPC analysis for **P-BB**, ¹H NMR spectroscopy confirmed the absence of aldehydic hydrogens characteristic of the monomer. ^dThermogravimetric analysis conducted under nitrogen; temperature reported upon 5% mass loss; residue (%) reported at end of TGA experiment. ^eAcidity of HFIP degraded the sample before GPC analysis of **D-BB**. Nonetheless, ¹H NMR spectroscopy confirmed the absence of aldehydic hydrogens characteristic of the monomer.

Gel Permeation Chromatography (GPC) Analysis (in hexafluoroisopropanol, HFIP)

Molecular Weight Averages

Peak	M _p	M _n	M _w	M _z	M _{z+1}	M _v	PD
Peak 1	22636	10601	23713	35982	49249	34180	2.237

Peak information

	Start (mins)	End (mins)
Baseline region 1	21.79	24.79
Baseline region 2	52.23	55.23
Peak 1	30.00	39.47

Peak	Trace	Peak Max RT (mins)	Peak Area (mV.s)	Peak Height (mV)
Peak 1	RI	33.96	8261878.103	36693.014

Chromatogram

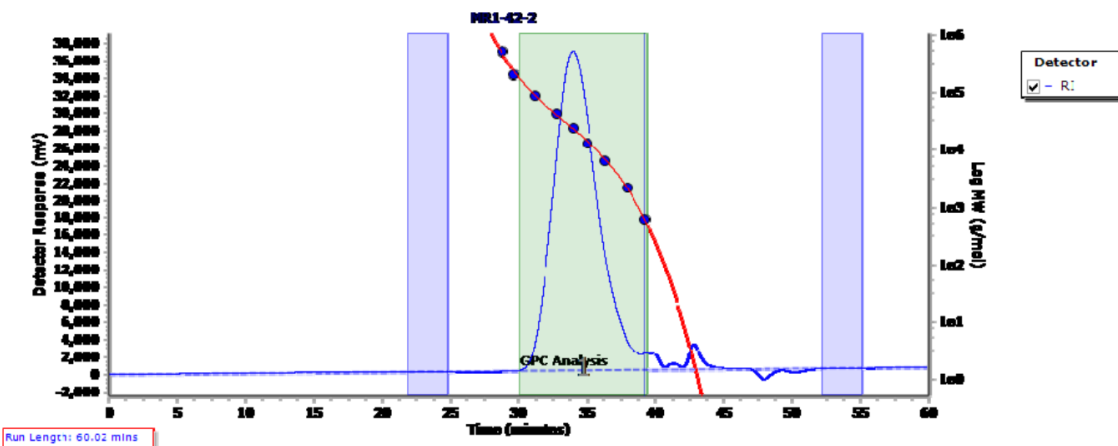


Figure S1. GPC Chromatogram of P-VV (Table S1, entry 2).

Molecular Weight Averages

Peak	M _p	M _n	M _w	M _z	M _{z+1}	M _v	PD
Peak 1	34555	18579	36007	55512	80338	52399	1.938

Peak information

	Start (mins)	End (mins)
Baseline region 1	19.68	25.37
Baseline region 2	45.55	48.58
Peak 1	28.84	38.43

Peak	Trace	Peak Max RT (mins)	Peak Area (mV.s)	Peak Height (mV)
Peak 1	RI	33.02	9732799.980	44984.223

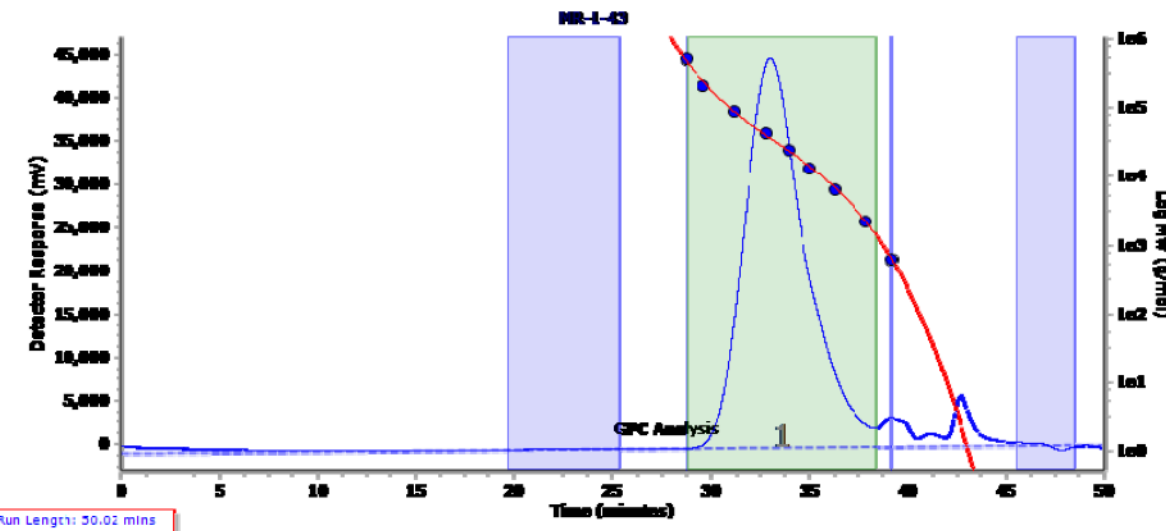
Chromatogram

Figure S2. GPC Chromatogram of P-SS (Table S1, entry 3).

Molecular Weight Averages

Peak	M _p	M _n	M _w	M _z	M _{z+1}	M _v	PD
Peak 1	40901	18469	47786	85802	141919	79217	2.587

Peak information

	Start (mins)	End (mins)
Baseline region 1	22.74	25.24
Baseline region 2	45.48	46.22
Peak 1	28.55	39.25

Peak	Trace	Peak Max RT (mins)	Peak Area (mV.s)	Peak Height (mV)
Peak 1	RI	32.66	8054002.391	31880.956

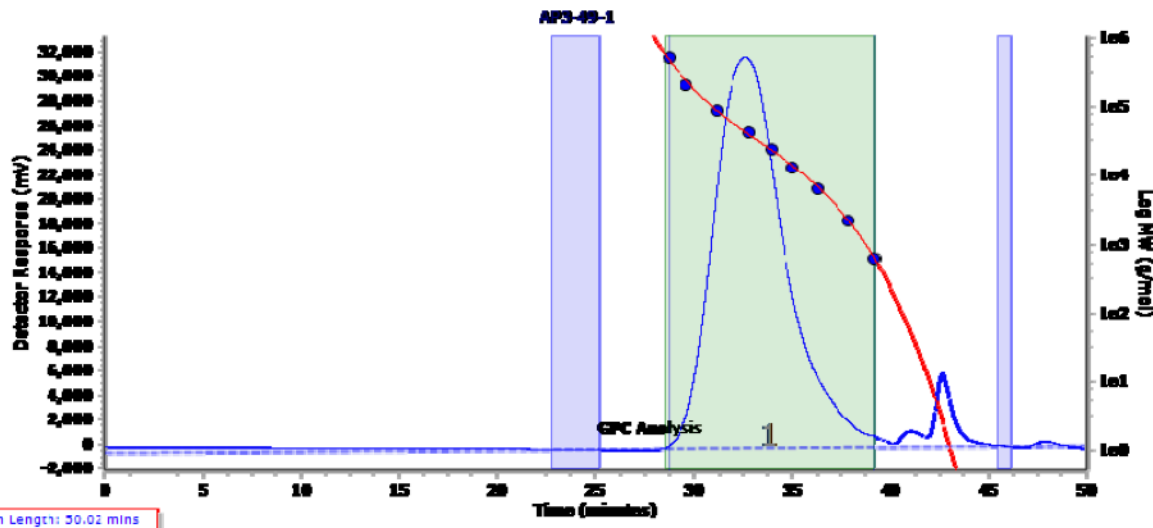
Chromatogram

Figure S3. GPC Chromatogram of P-EE (Table S1, entry 4).

Molecular Weight Averages

Peak	M _p	M _n	M _w	M _z	M _{z+1}	M _v	PD
Peak 1	2555	2569	3504	4763	6111	4567	1.364

Peak information

	Start (mins)	End (mins)
Baseline region 1	21.24	24.24
Baseline region 2	52.68	55.68
Peak 1	34.85	38.62

Peak	Trace	Peak Max RT (mins)	Peak Area (mV.s)	Peak Height (mV)
Peak 1	RI	37.66	239429.903	1979.690

Chromatogram

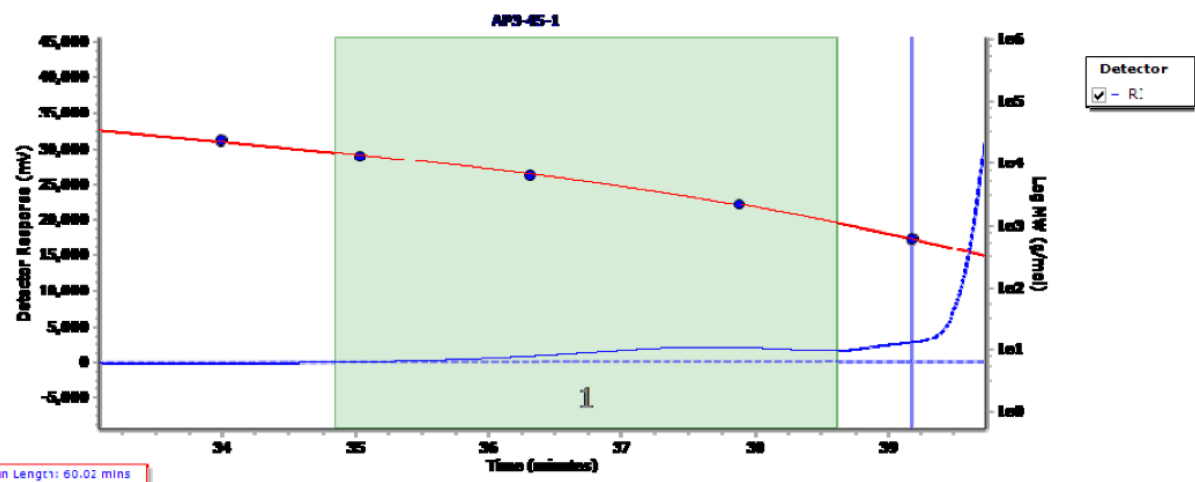


Figure S4. GPC Chromatogram of D-BB (Table S1, entry 5).

Molecular Weight Averages

Peak	M _p	M _n	M _w	M _z	M _{z+1}	M _v	PD
Peak 1	34713	22246	44198	78090	129686	72046	1.987

Peak information

	Start (mins)	End (mins)
Baseline region 1	20.42	23.42
Baseline region 2	55.70	58.70
Peak 1	28.67	37.65

Peak	Trace	Peak Max RT (mins)	Peak Area (mV.s)	Peak Height (mV)
Peak 1	RI	33.02	13751703.772	56737.240

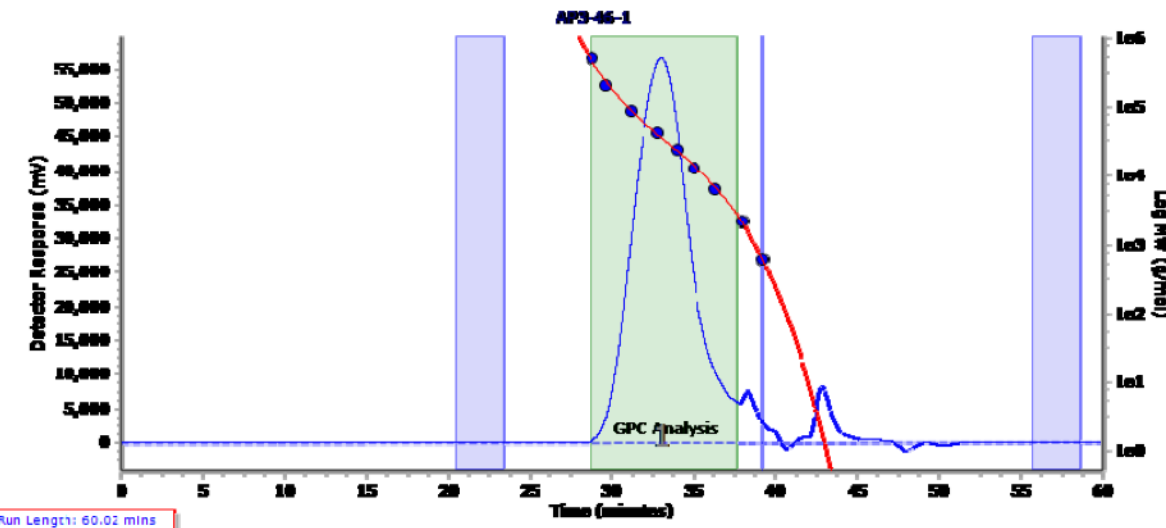
Chromatogram

Figure S5. GPC Chromatogram of D-VV (Table S1, entry 6).

Molecular Weight Averages

Peak	M _p	M _n	M _w	M _z	M _{z+1}	M _v	PD
Peak 1	28989	21590	34623	50968	71673	48305	1.604

Peak information

	Start (mins)	End (mins)
Baseline region 1		22.28
Baseline region 2		55.43
Peak 1	29.41	37.43

Peak	Trace	Peak Max RT (mins)	Peak Area (mV.s)	Peak Height (mV)
Peak 1	RI	33.41	10001500.829	47844.869

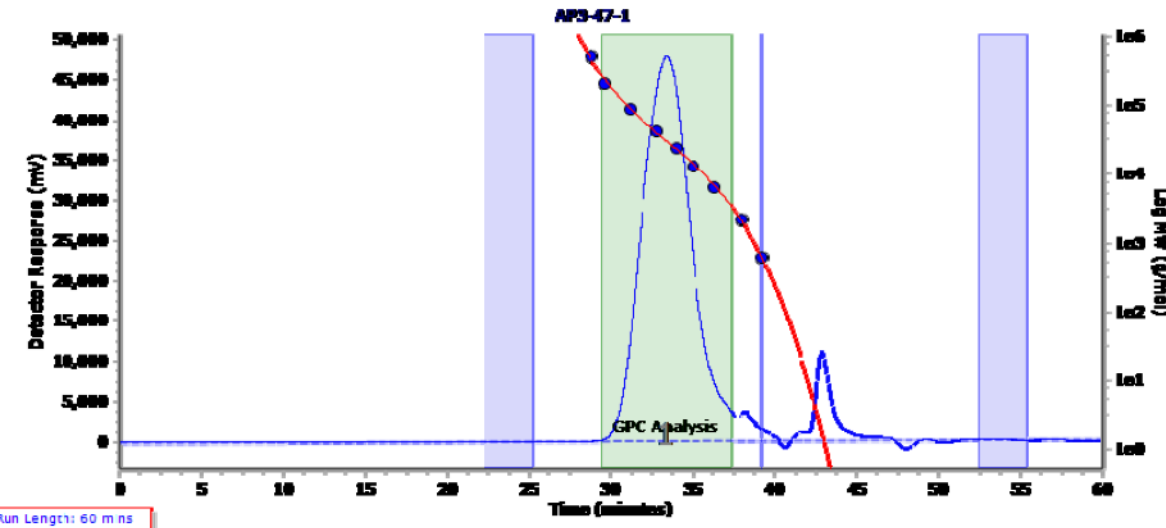
Chromatogram

Figure S6. GPC Chromatogram of D-SS (Table S1, entry 7).

Molecular Weight Averages

Peak	M _p	M _n	M _w	M _z	M _{z+1}	M _v	PD
Peak 1	36337	19263	42066	75095	124241	69396	2.184

Peak information

	Start (mins)	End (mins)
Baseline region 1	21.79	24.79
Baseline region 2	55.31	58.31
Peak 1	28.46	37.85

Peak	Trace	Peak Max RT (mins)	Peak Area (mV.s)	Peak Height (mV)
Peak 1	RI	32.91	7522303.056	28981.610

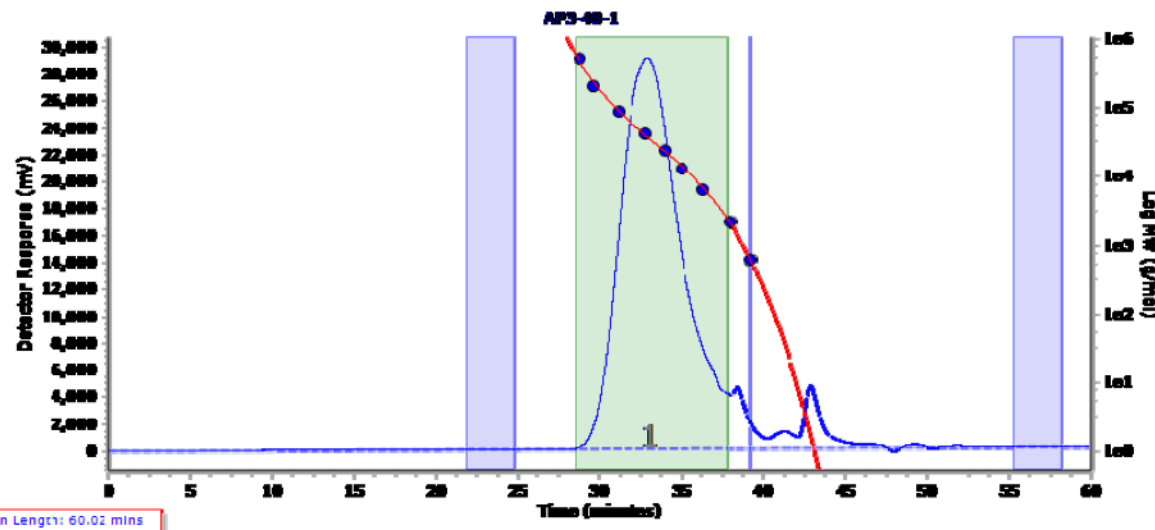
Chromatogram

Figure S7. GPC Chromatogram of D-EE (Table S1, entry 8).

Differential Scanning Calorimetry (DSC) Thermograms

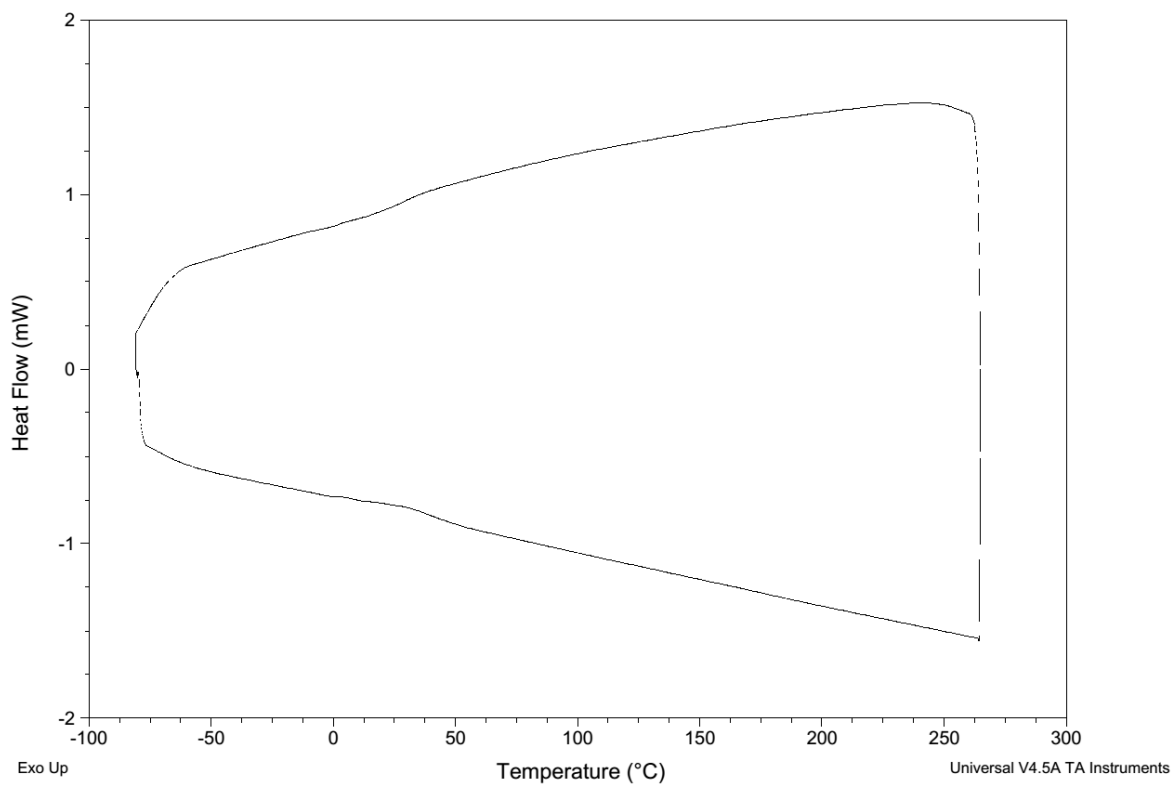


Figure S8. DSC Thermogram of P-BB (Table S1, entry 1).

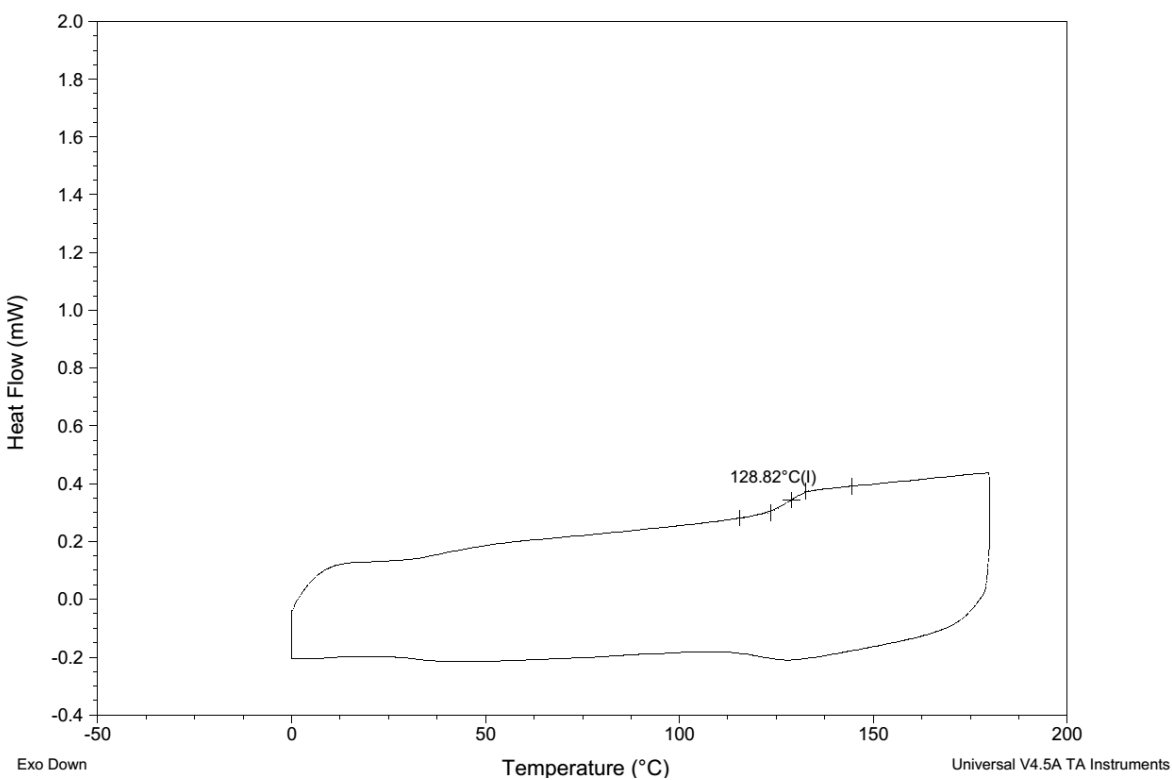


Figure S9. DSC Thermogram of P-VV (Table S1, entry 2).

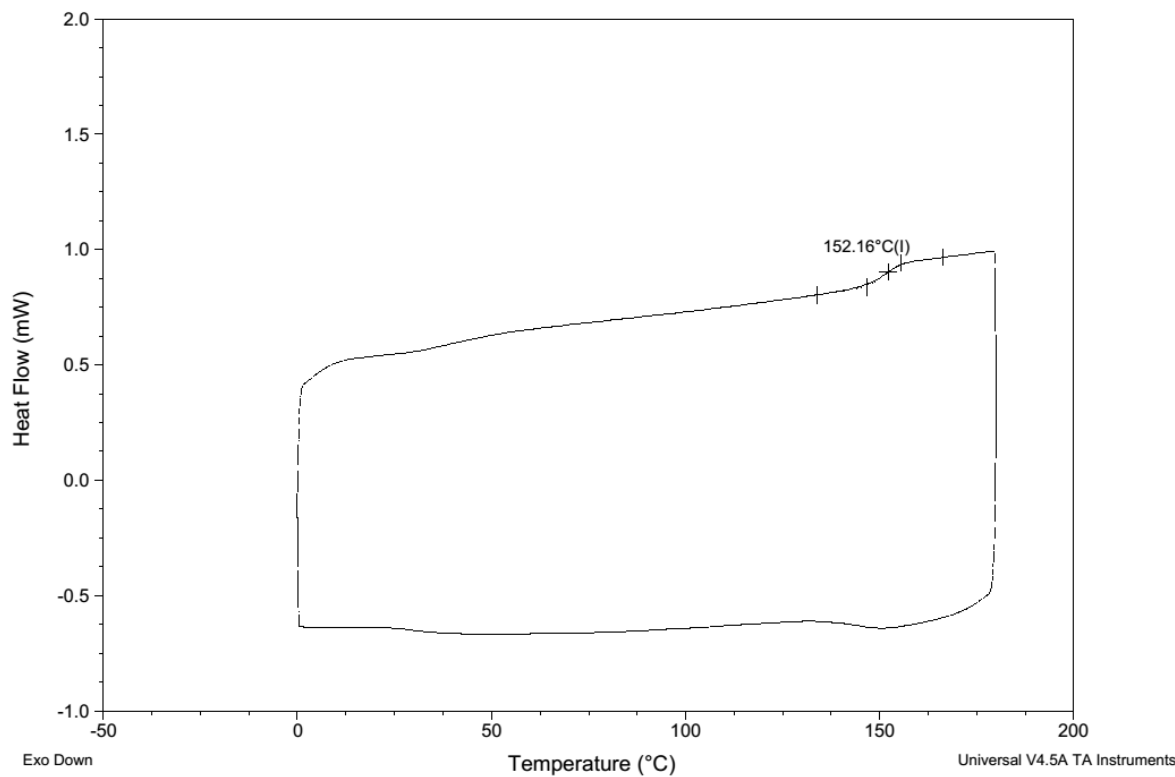


Figure S10. DSC Thermogram of **P-SS** (Table S1, entry 3).

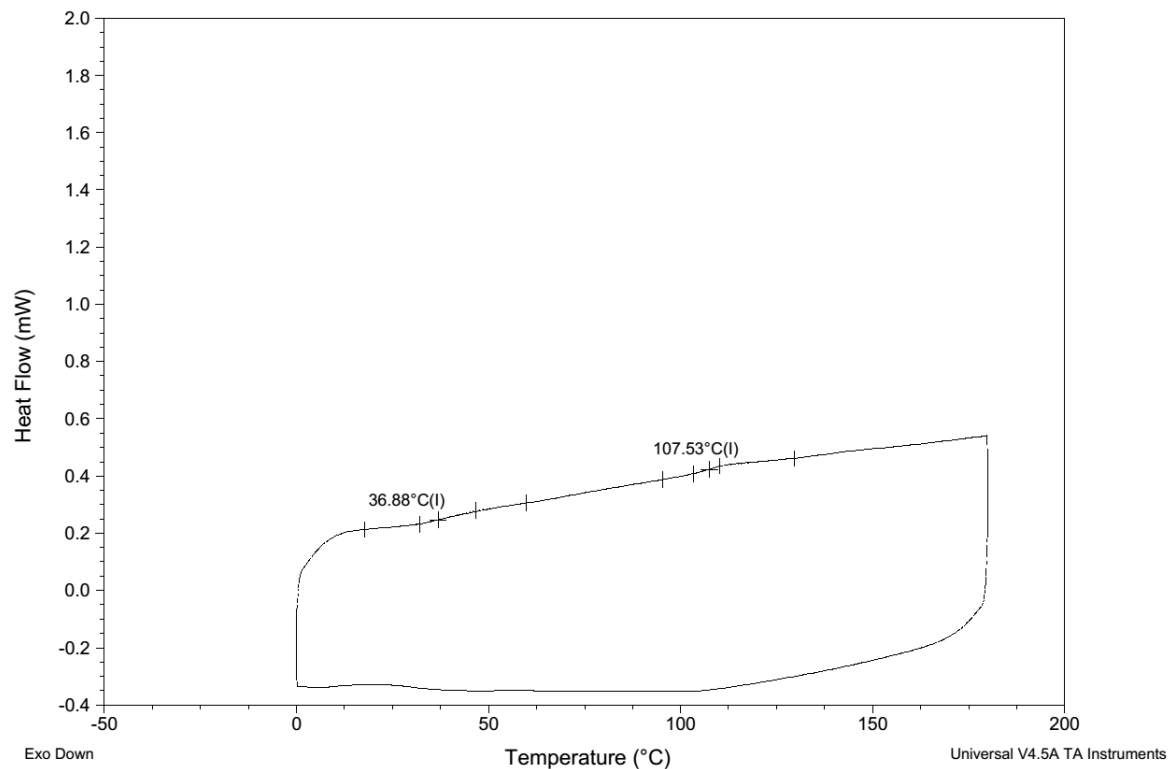


Figure S11. DSC Thermogram of **P-EE** (Table S1, entry 4).

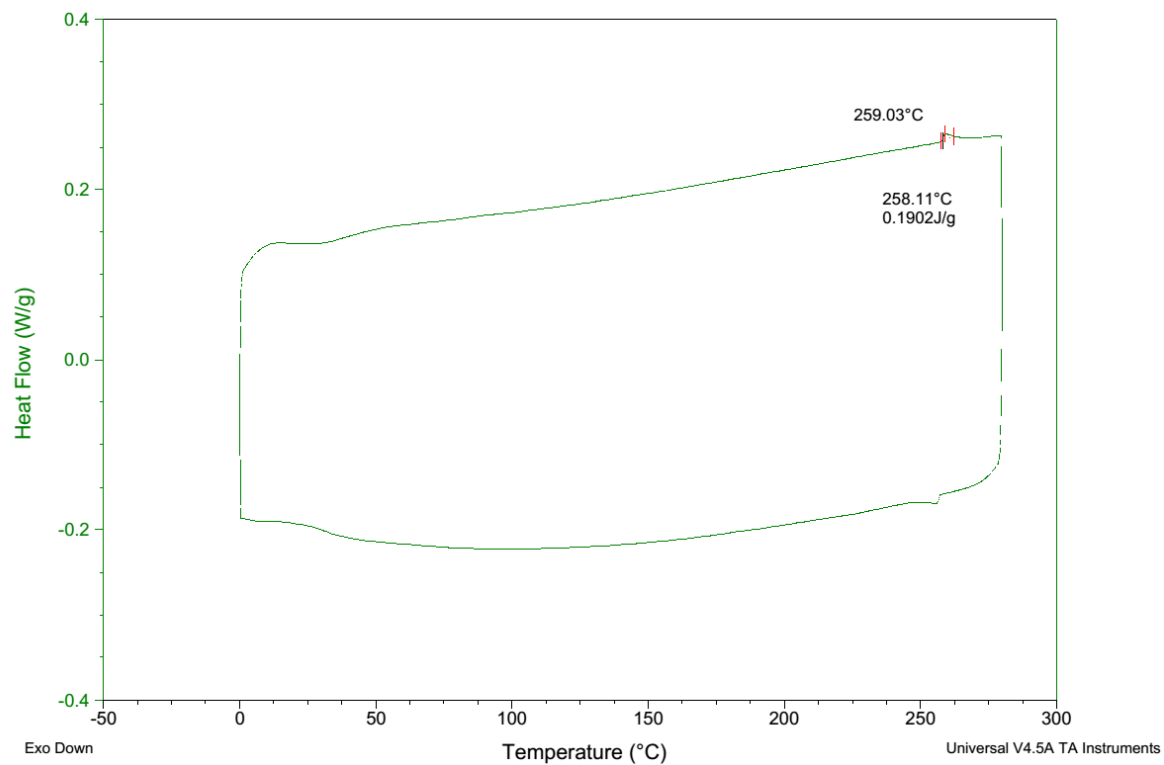


Figure S12. DSC Thermogram of **D-BB** (Table S1, entry 5).

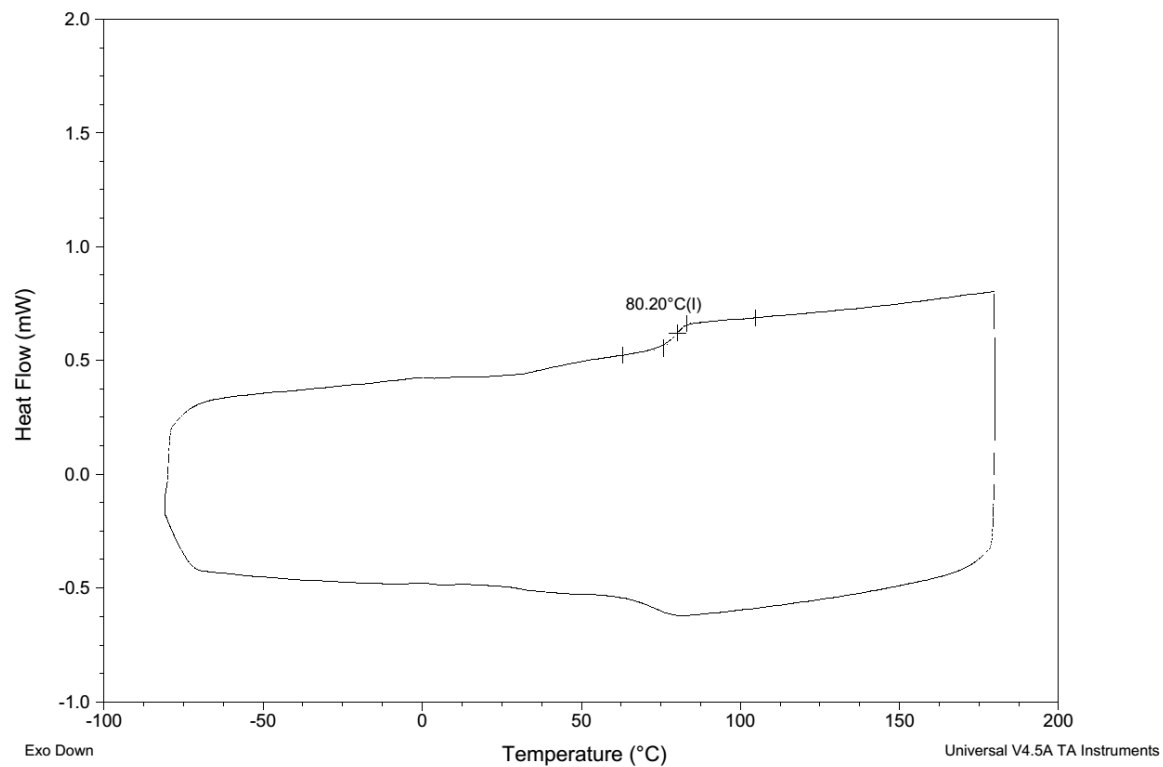


Figure S13. DSC Thermogram of **D-VV** (Table S1, entry 6).

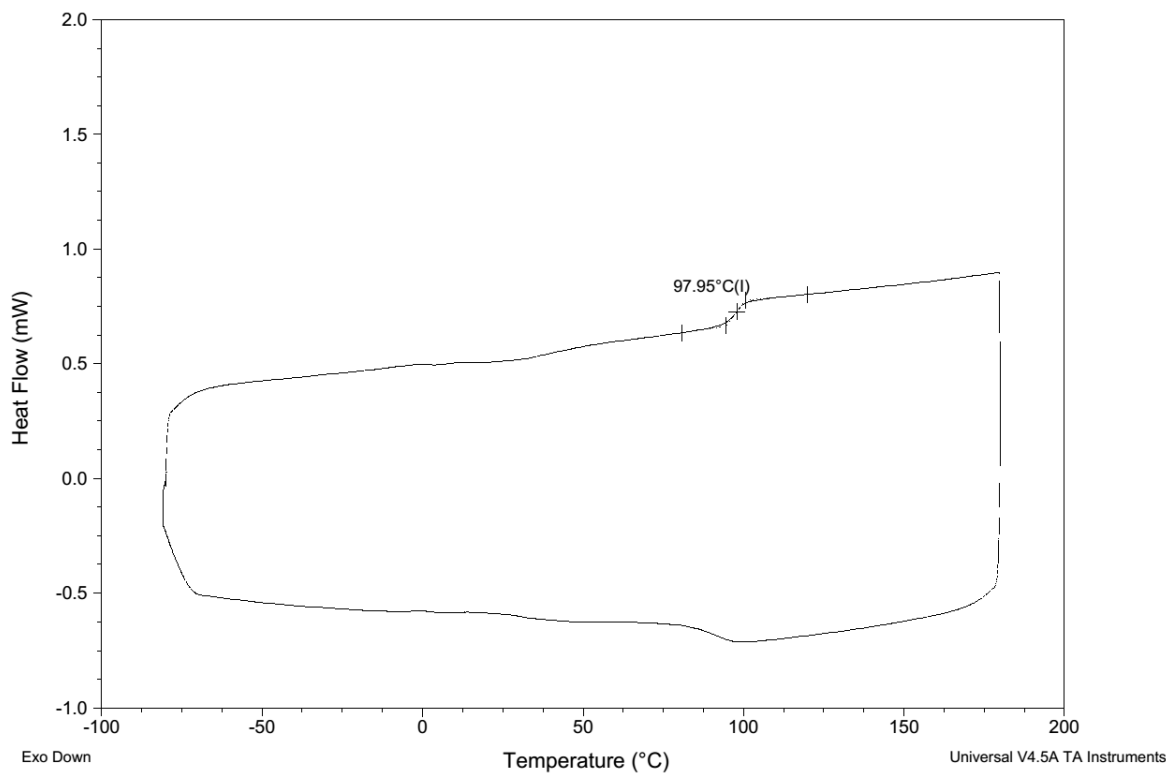


Figure S14. DSC Thermogram of D-SS (Table S1, entry 7).

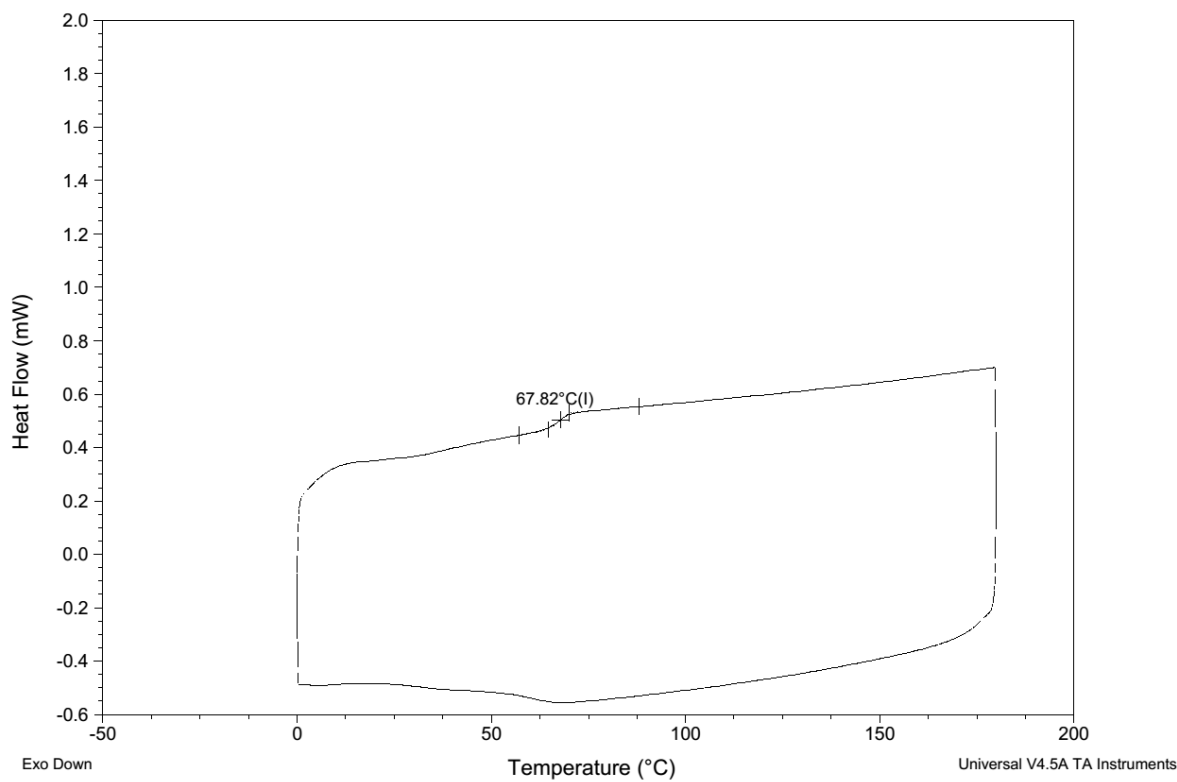


Figure S15. DSC Thermogram of D-EE (Table S1, entry 8).

Thermogravimetric Analysis (TGA) Thermograms

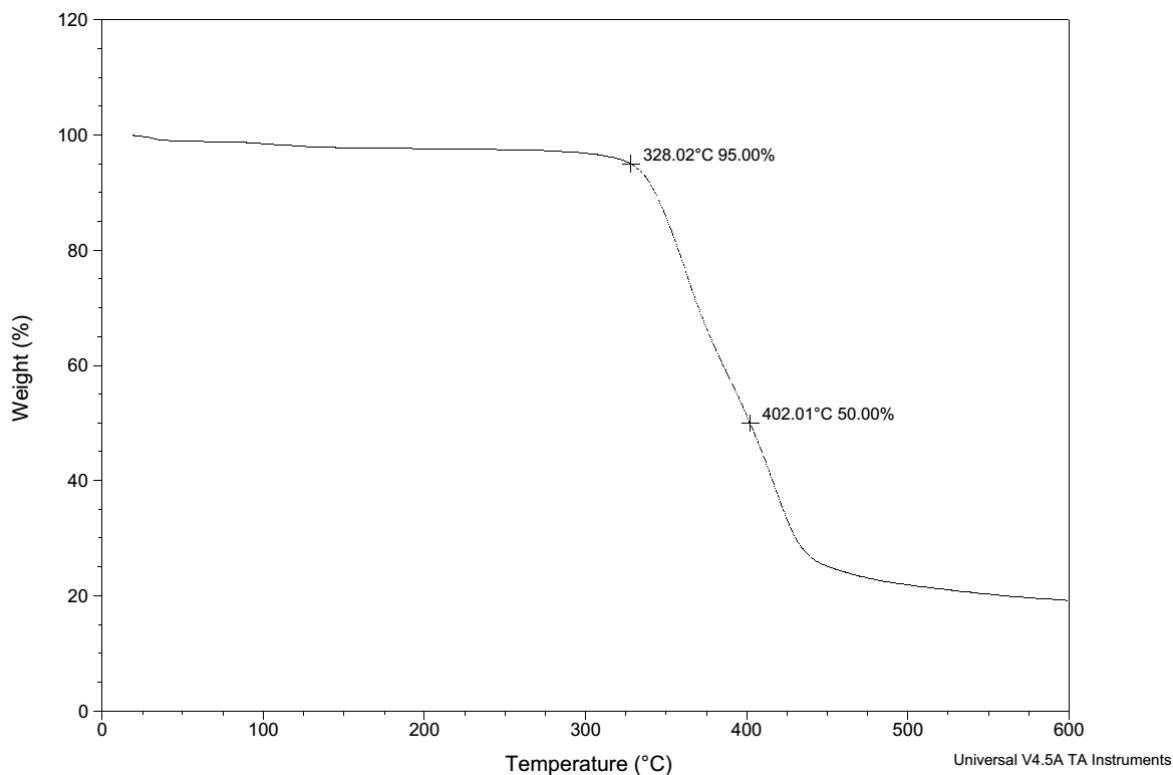


Figure S16. TGA Thermogram of **P-BB** (Table S1, entry 1).

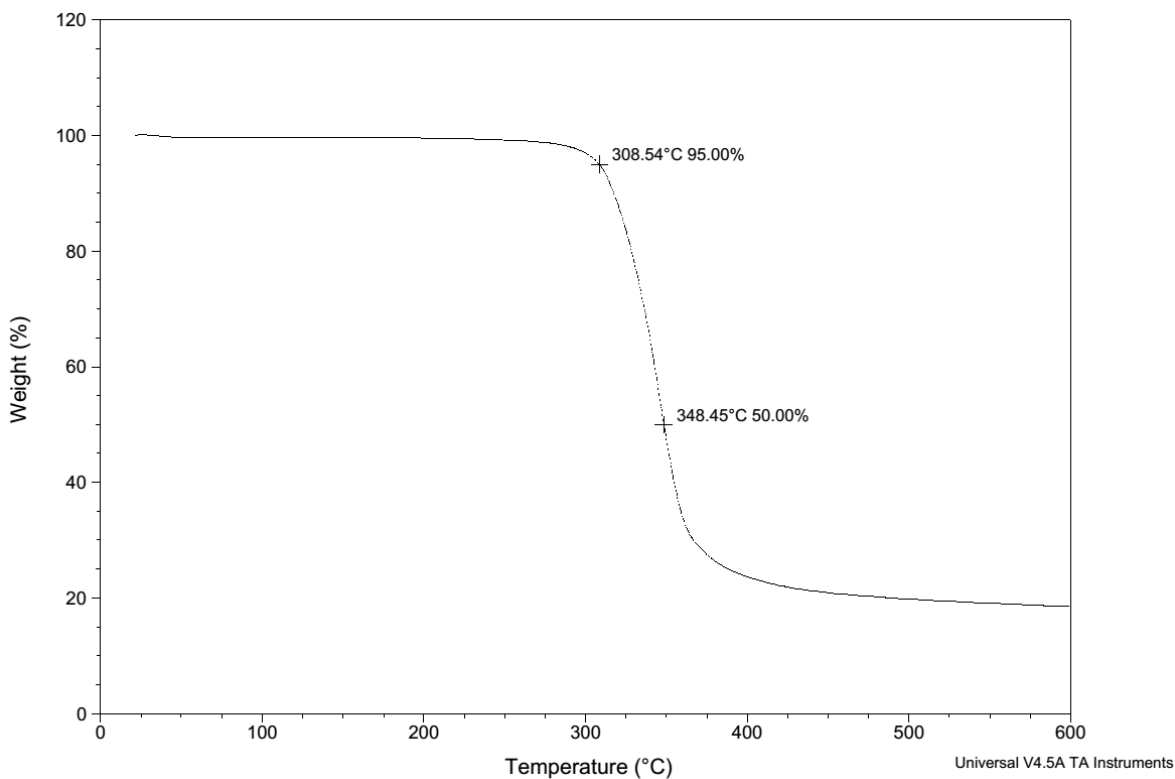


Figure S17. TGA Thermogram of **P-VV** (Table S1, entry 2).

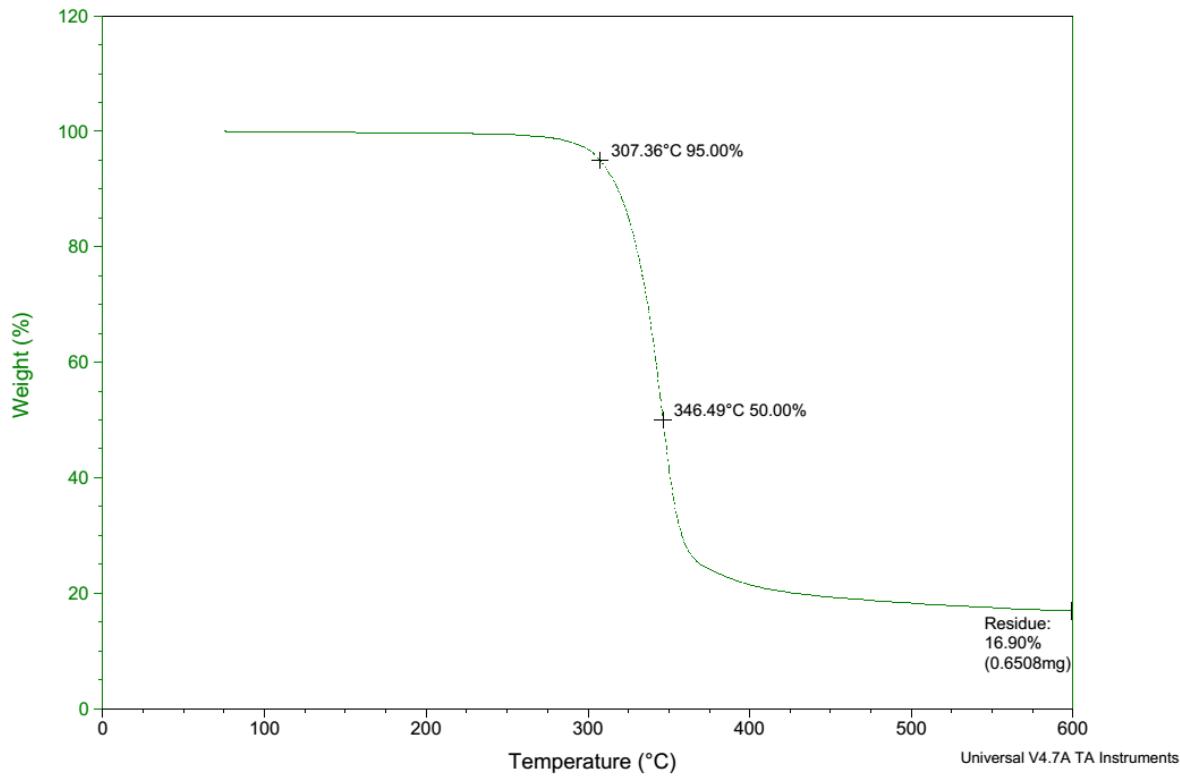


Figure S18. TGA Thermogram of P-SS (Table S1, entry 3).

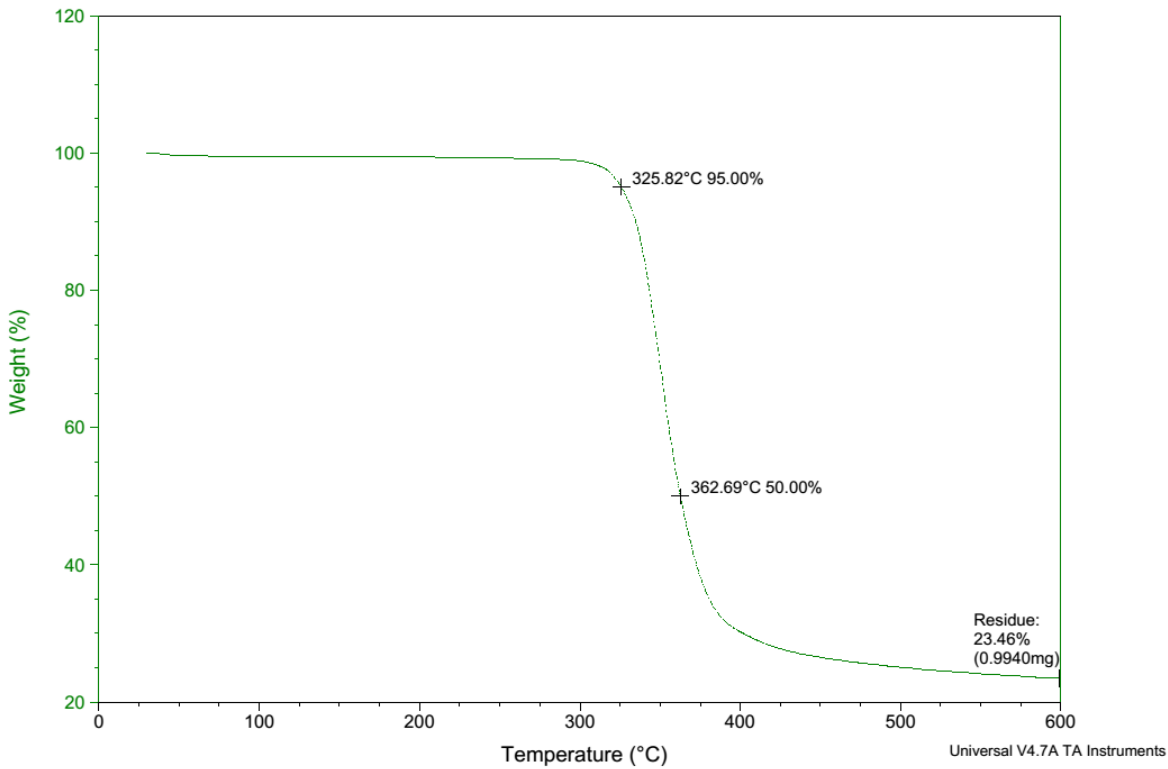


Figure S19. TGA Thermogram of P-EE (Table S1, entry 4).

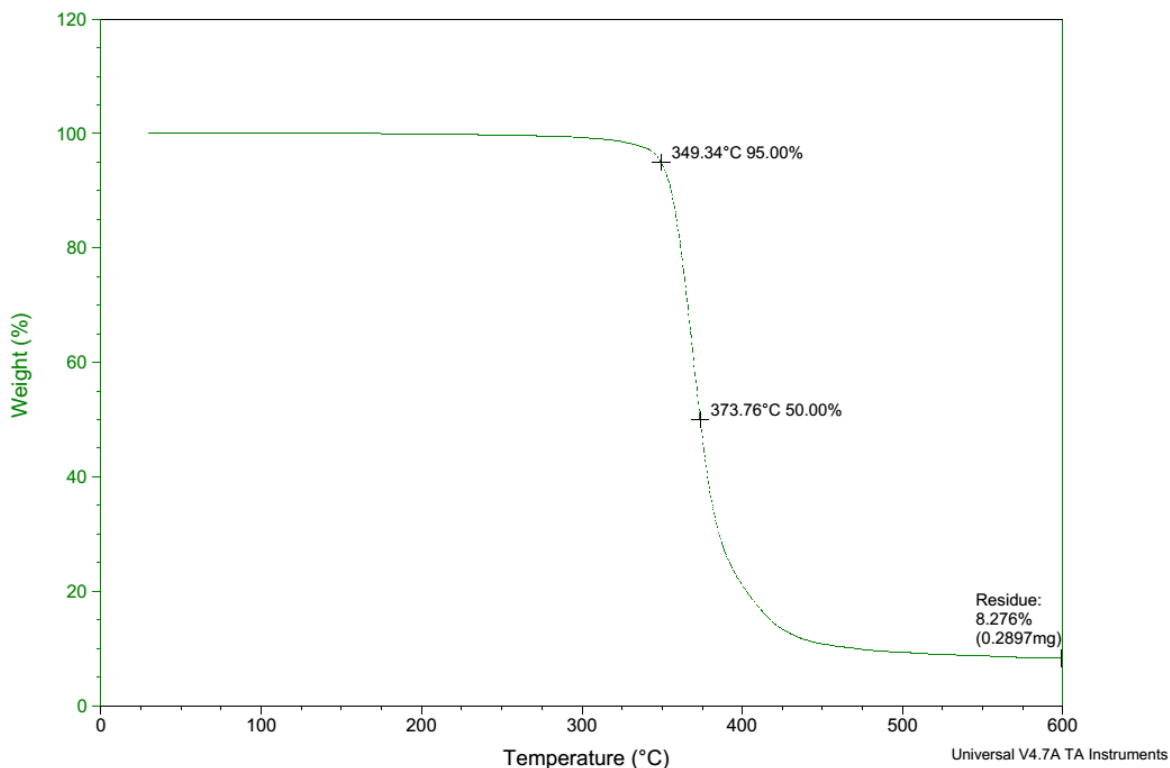


Figure S20. TGA Thermogram of **D-BB** (Table S1, entry 5).

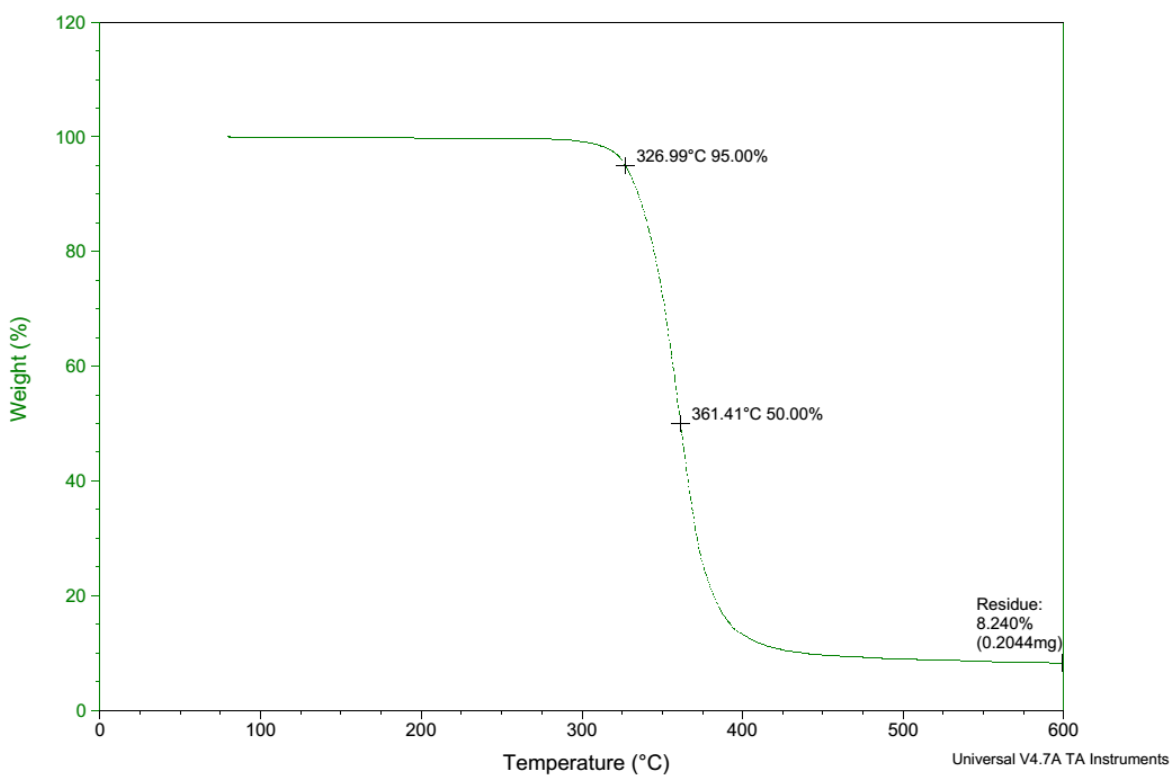


Figure S21. TGA Thermogram of **D-VV** (Table S1, entry 6).

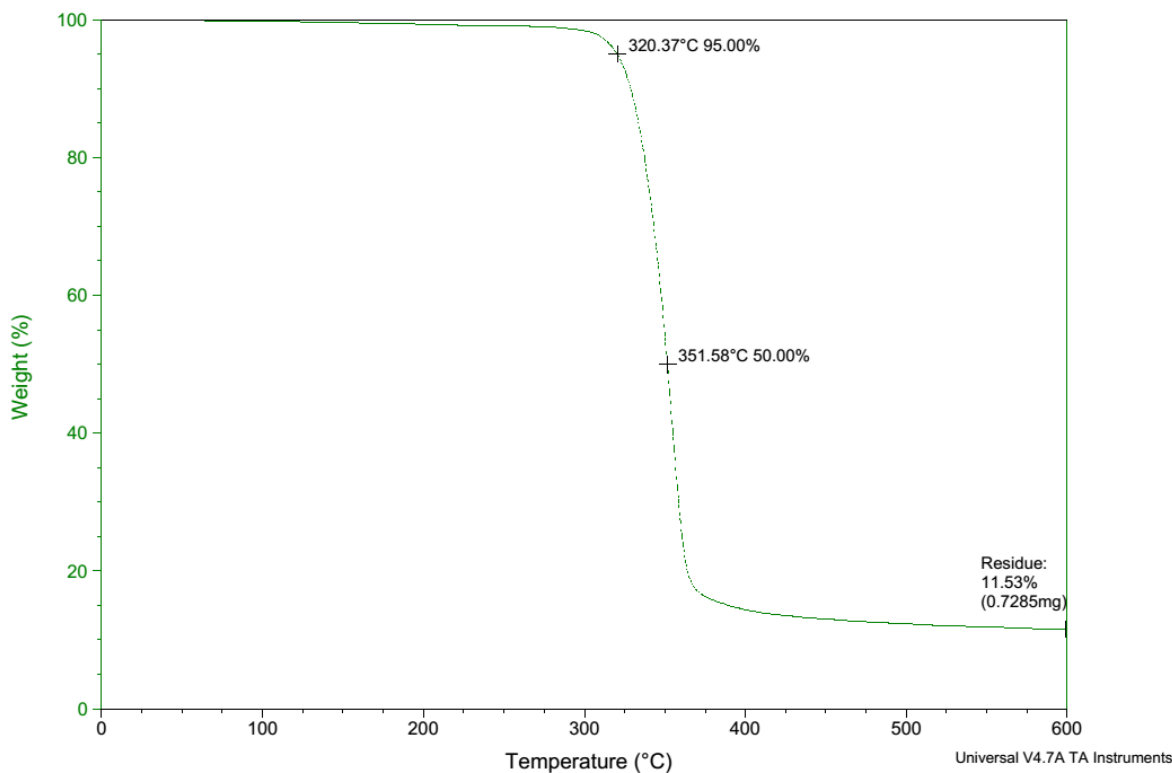


Figure S22. TGA Thermogram of **D-SS** (Table S1, entry 7).

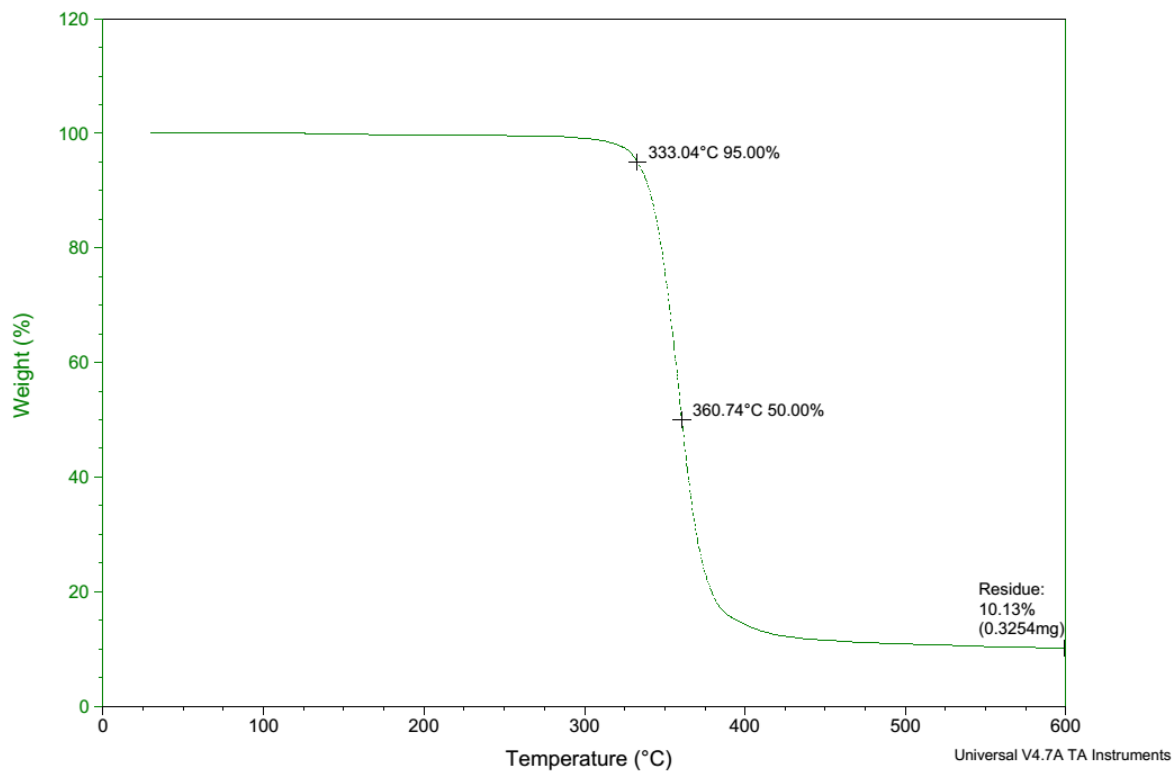


Figure S23. TGA Thermogram of **D-EE** (Table S1, entry 8).

¹H NMR Spectra

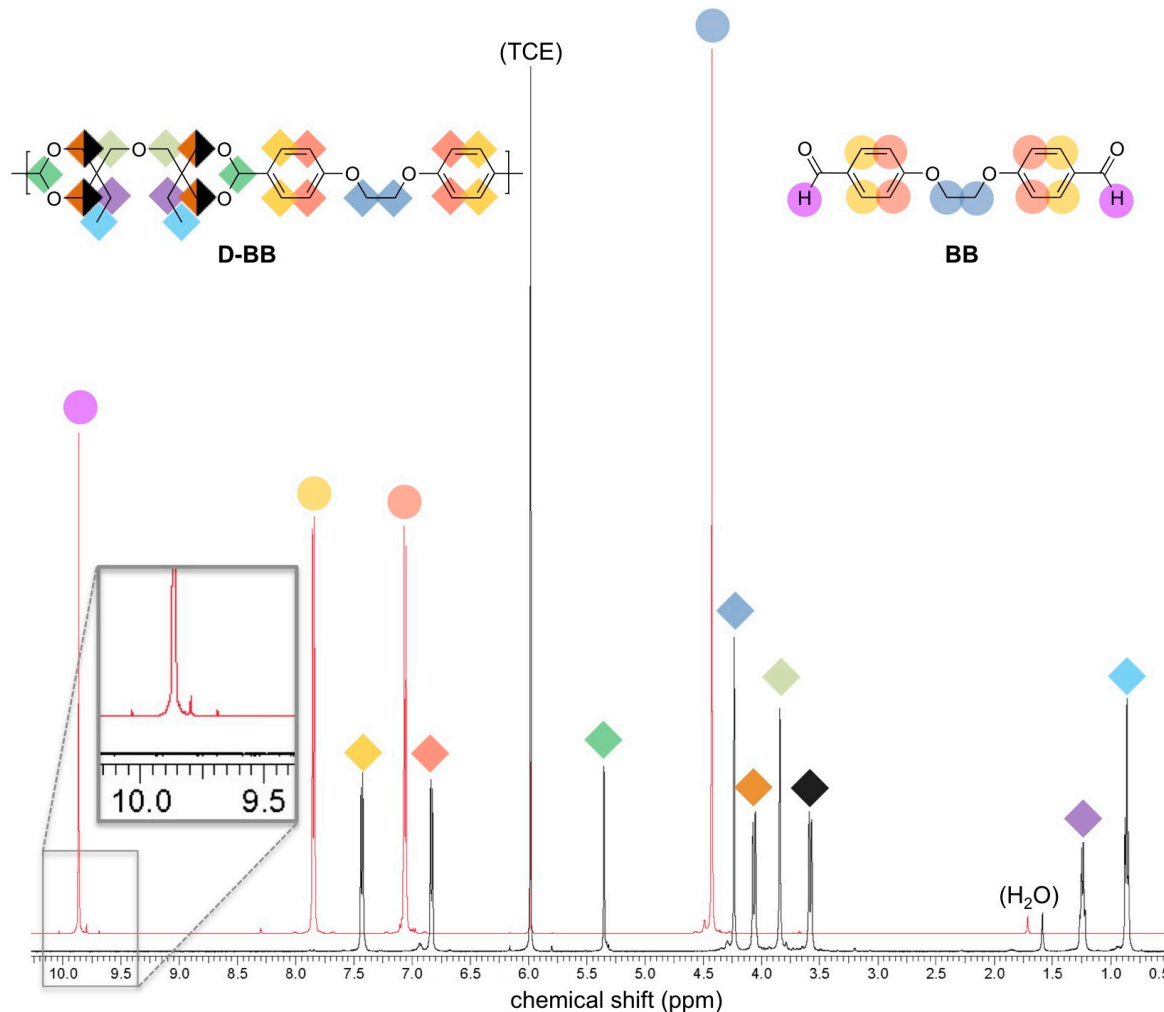


Figure S24. ¹H NMR spectra of **BB** (top, red trace) and **D-BB** (black, bottom trace) in TCE-*d*₂. Absence of the aldehydic proton (ca. 10 ppm) in the **D-BB** trace suggests that the monomer (**BB**) has been completely consumed and has been converted to high molecular weight polymer.

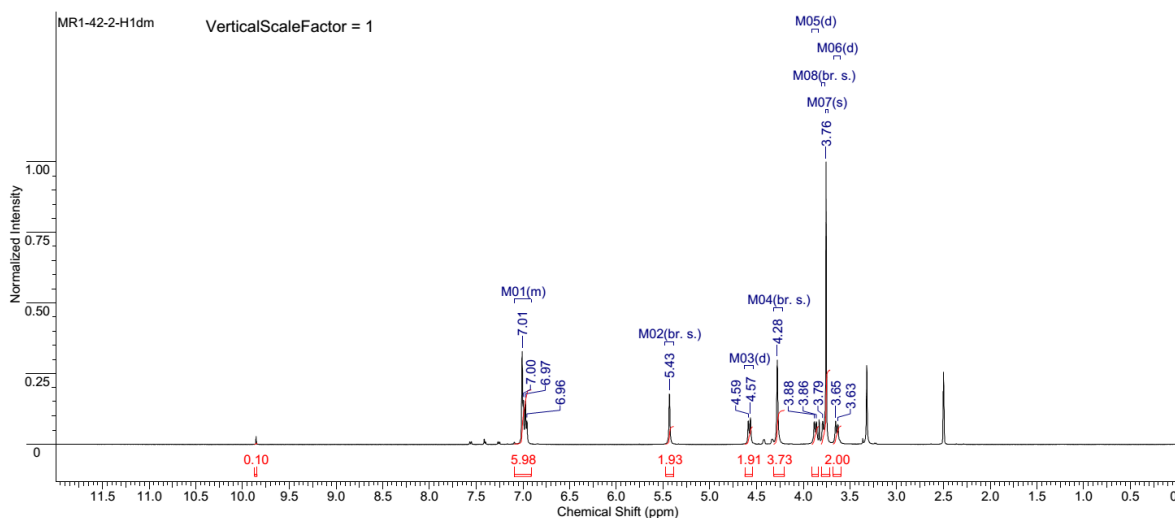


Figure S25. ¹H NMR spectrum of **P-VV** in DMSO-*d*₆ (Table S1, entry 2).

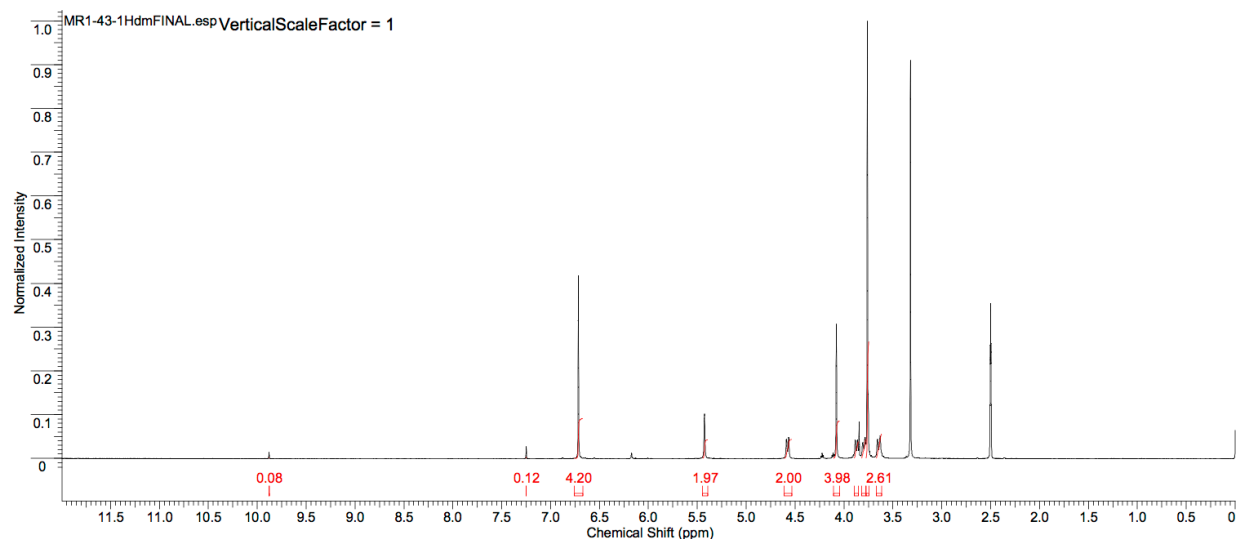


Figure S26. ^1H NMR spectrum of **P-SS** in $\text{DMSO}-d_6$ (Table S1, entry 3).

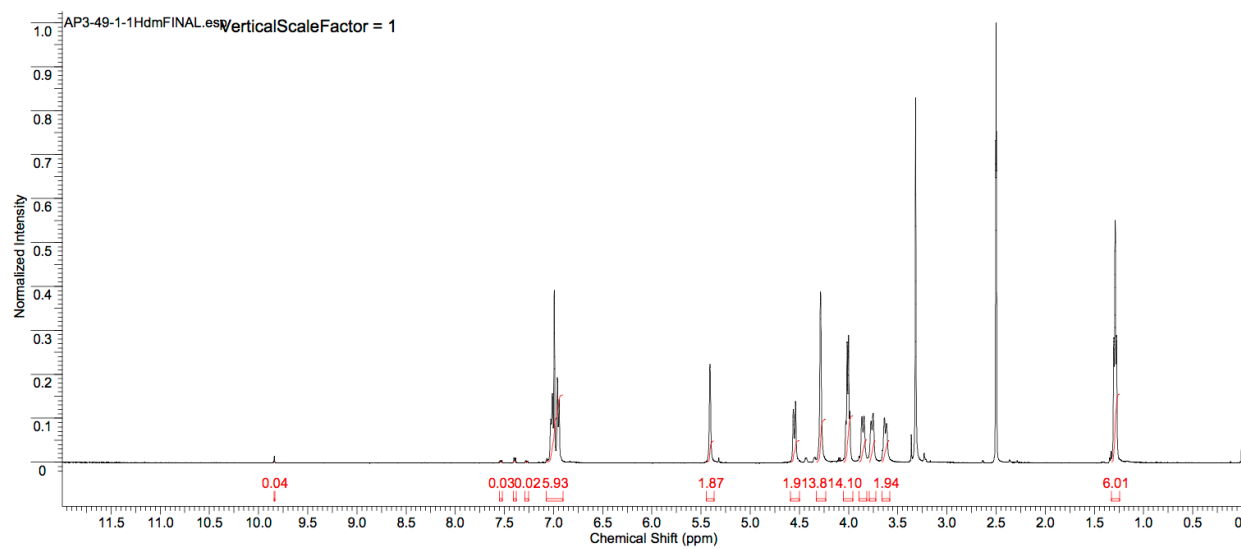


Figure S27. ^1H NMR spectrum of **P-EE** in $\text{DMSO}-d_6$ (Table S1, entry 4).

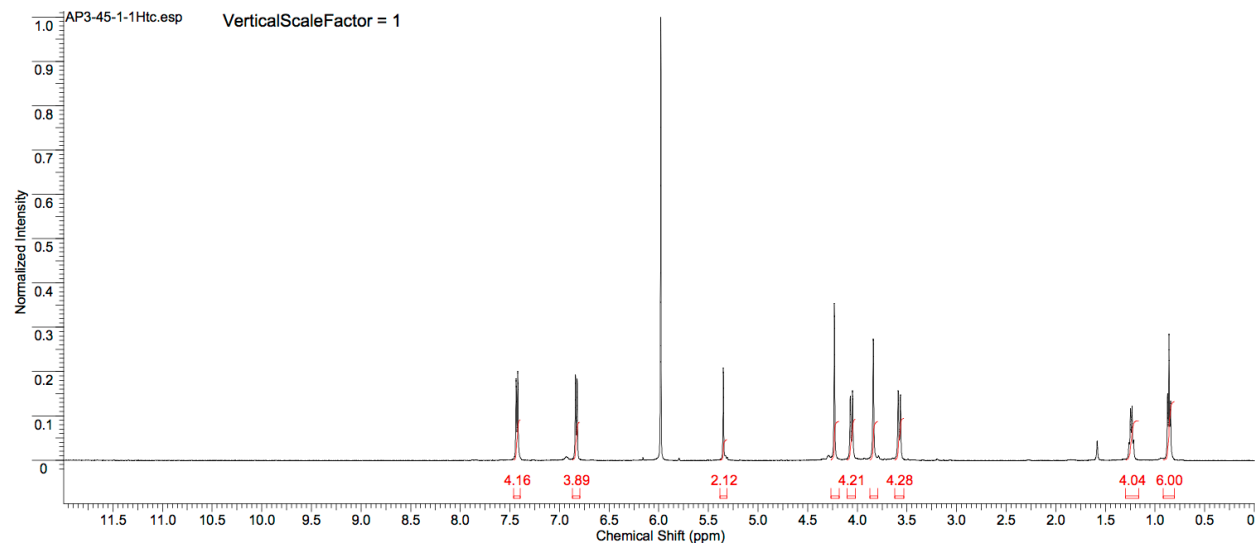


Figure S28. ^1H NMR spectrum of **D-BB** in $\text{TCE}-d_2$ (Table S1, entry 5).

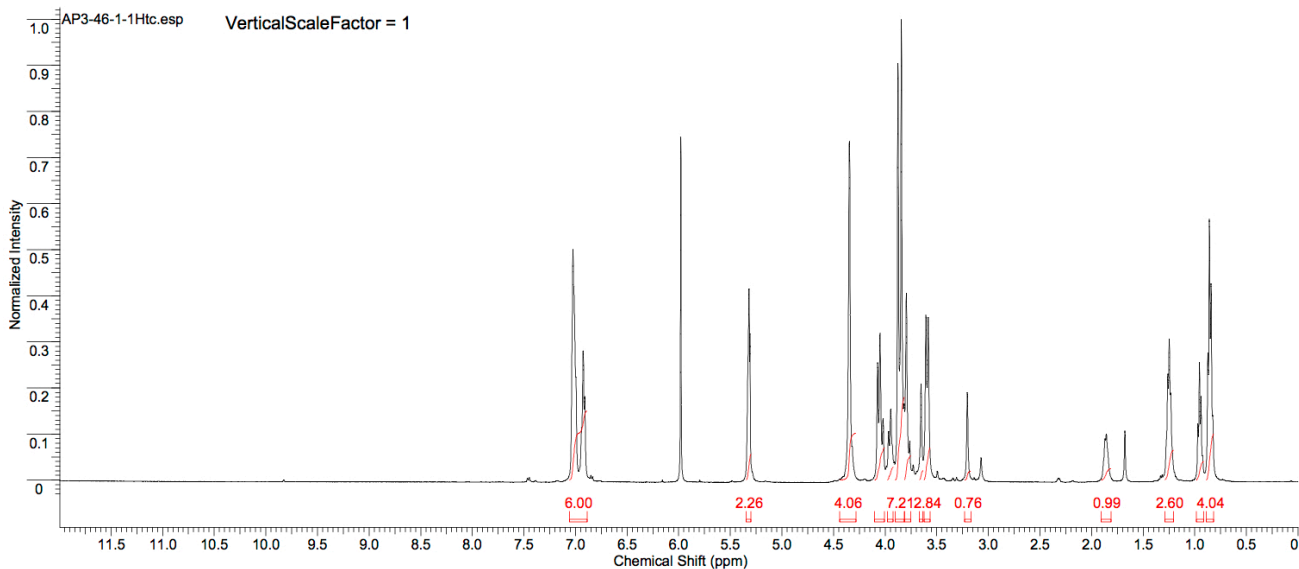


Figure S29. ^1H NMR spectrum of **D-VV** in $\text{TCE}-d_2$ (Table S1, entry 6).

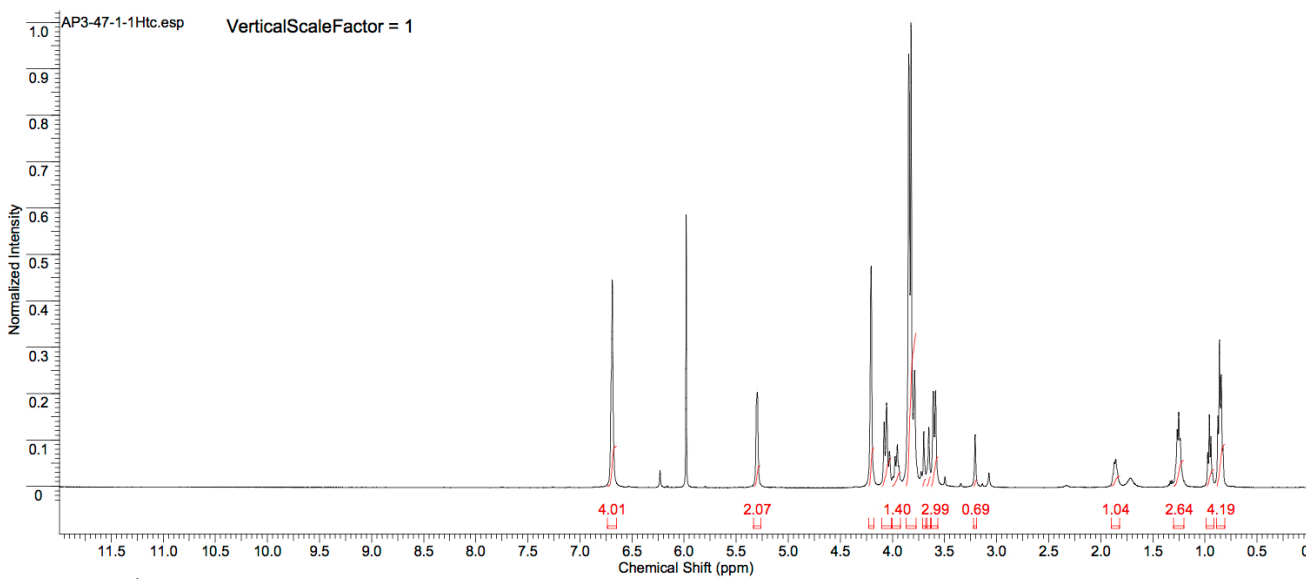


Figure S30. ^1H NMR spectrum of **D-SS** in $\text{TCE}-d_2$ (Table S1, entry 7).

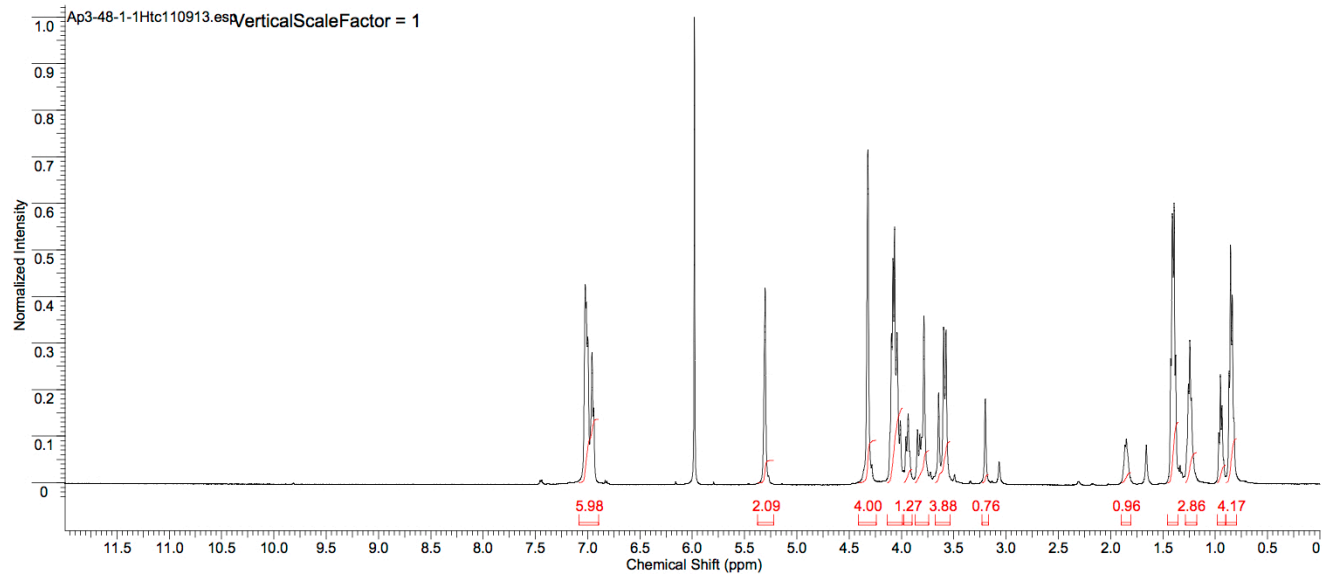


Figure S31. ^1H NMR spectrum of **D-EE** in $\text{TCE}-d_2$ (Table S1, entry 8).

¹³C NMR Spectra

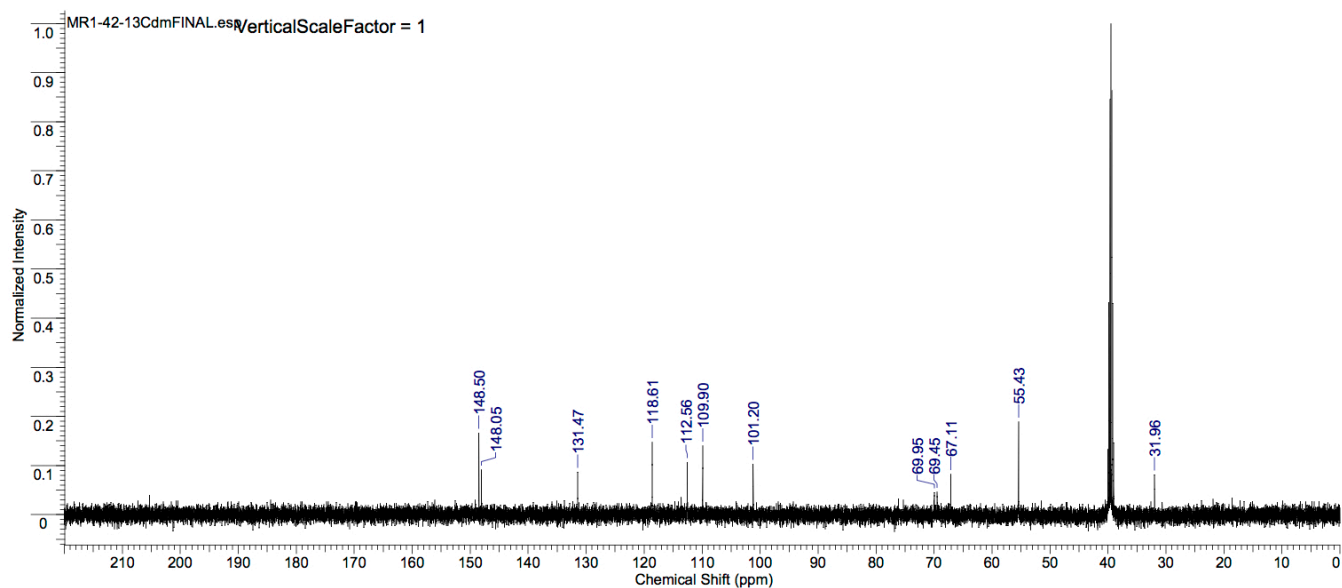


Figure S32. ¹³C NMR spectrum of P-VV in DMSO-*d*₆ (Table S1, entry 2).

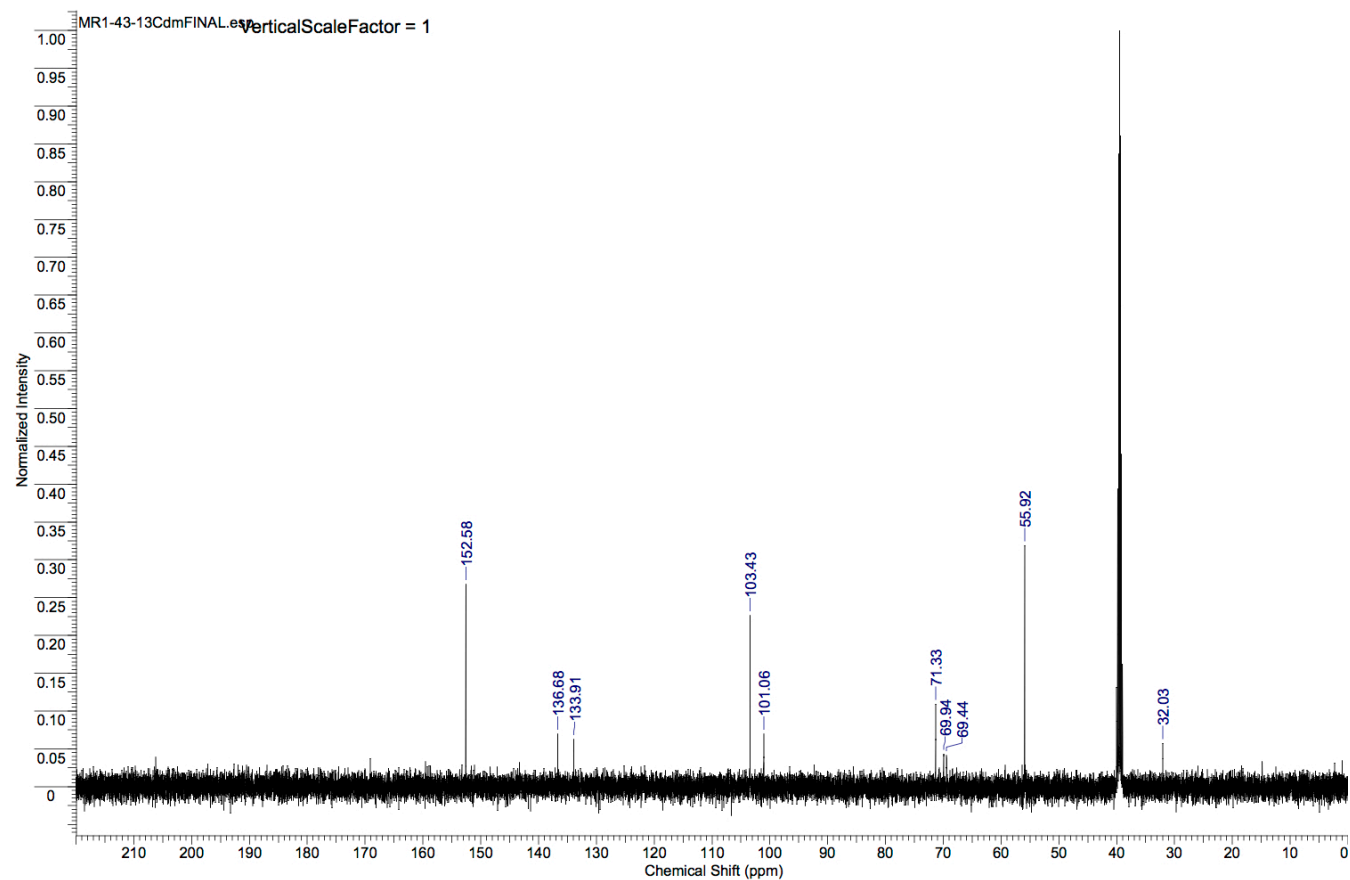


Figure S33. ¹³C NMR spectrum of P-SS in DMSO-*d*₆ (Table S1, entry 3).

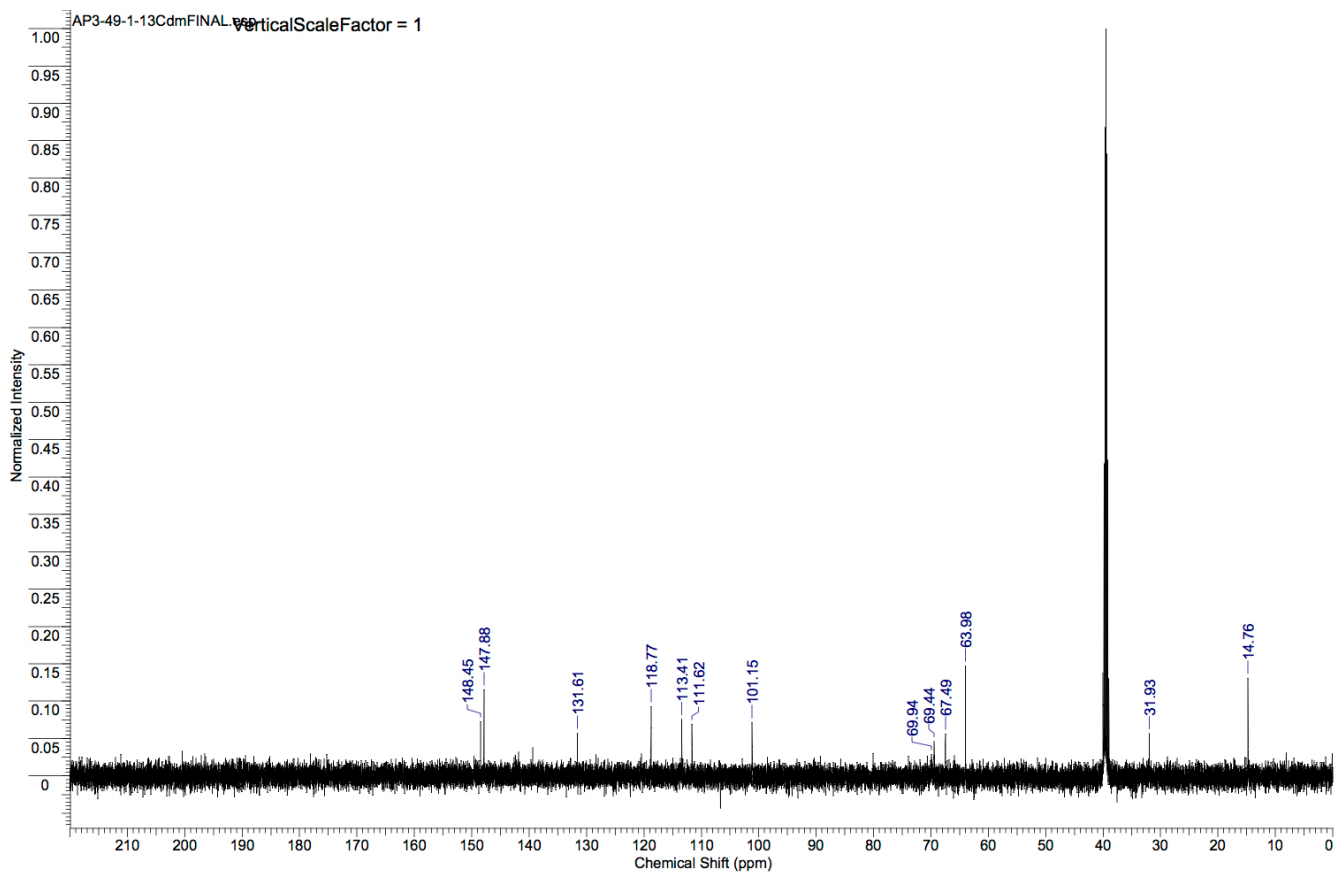


Figure S34. ^{13}C NMR spectrum of **P-EE** in $\text{DMSO}-d_6$ (Table S1, entry 4).

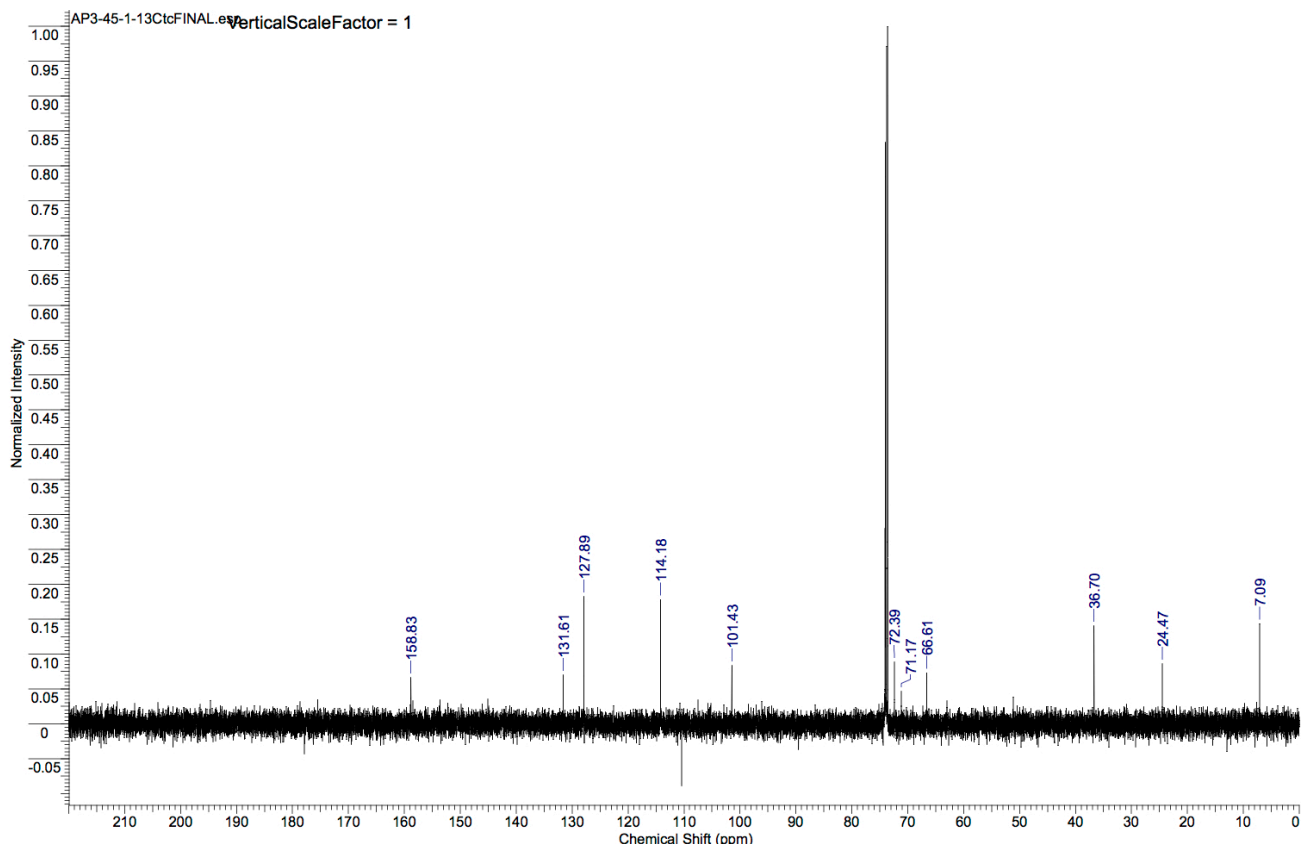


Figure S35. ^{13}C NMR spectrum of **D-BB** in $\text{TCE}-d_2$ (Table S1, entry 5).

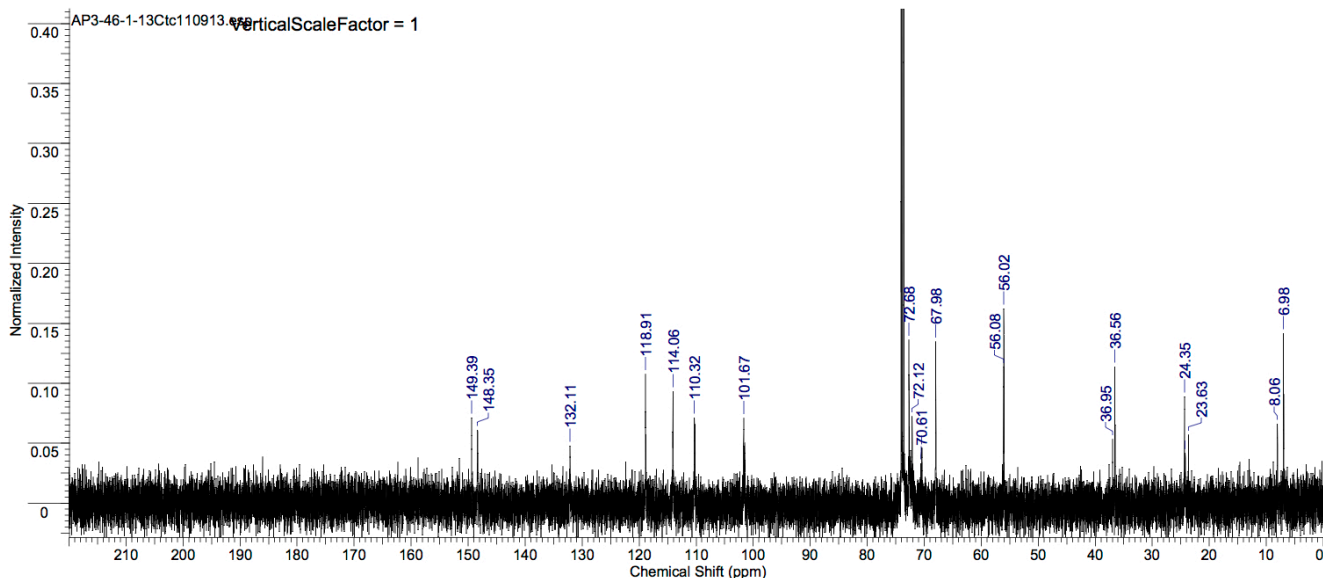


Figure S36. ^{13}C NMR spectrum of **D-VV** in $\text{TCE}-d_2$ (Table S1, entry 6).

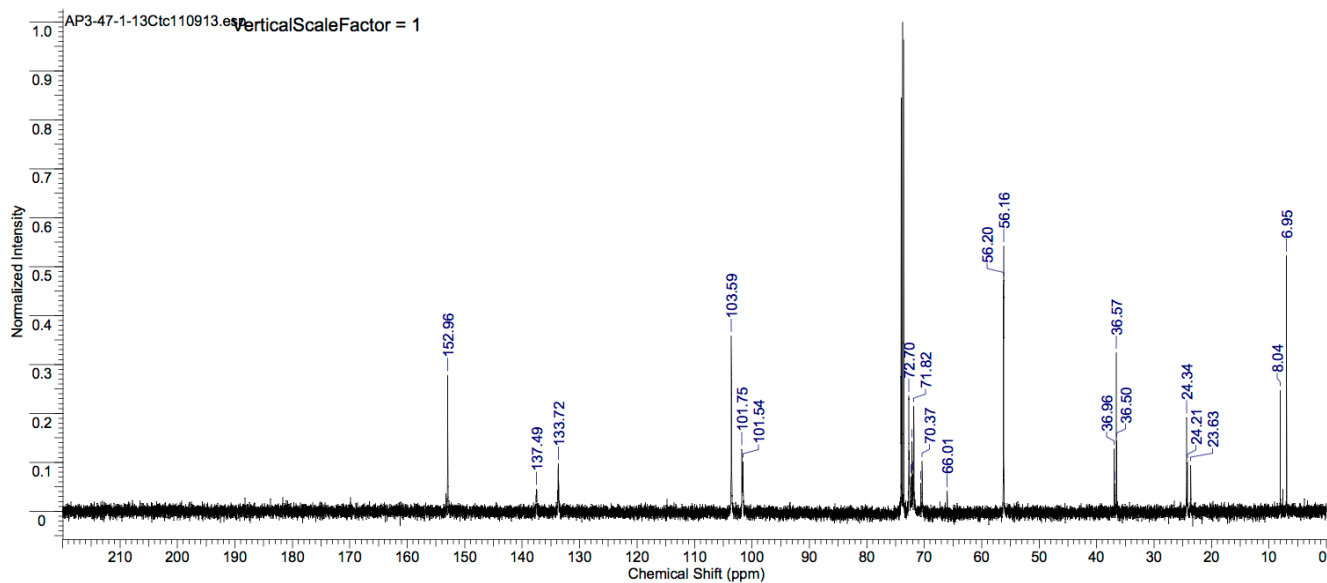


Figure S37. ^{13}C NMR spectrum of **D-SS** in $\text{TCE}-d_2$ (Table S1, entry 7).

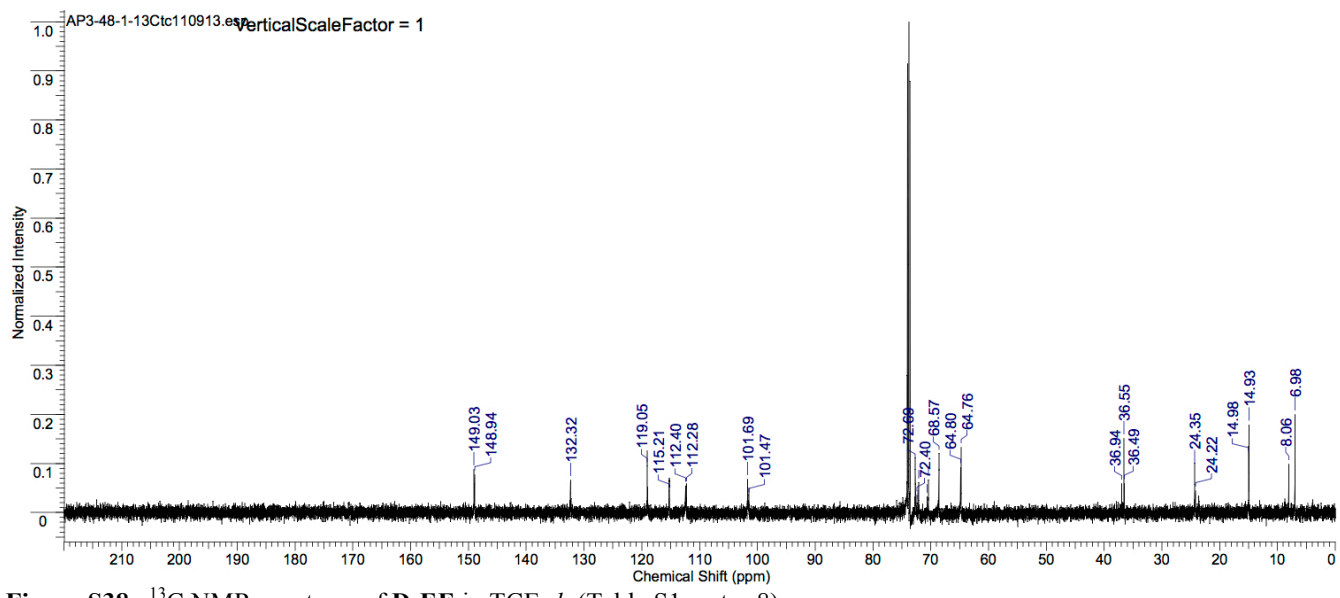


Figure S38. ^{13}C NMR spectrum of **D-EE** in $\text{TCE}-d_2$ (Table S1, entry 8).

Fourier Transform Infrared Spectroscopy (FTIR) Spectra

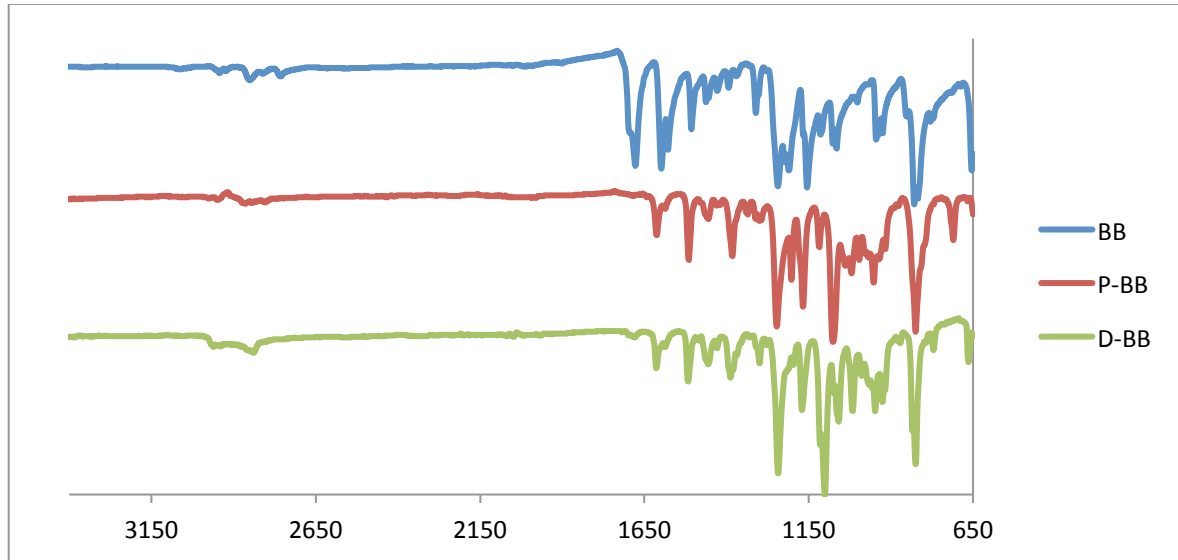


Figure S39. Comparative FTIR spectra for **BB** (monomer), **P-BB**, and **D-BB**.

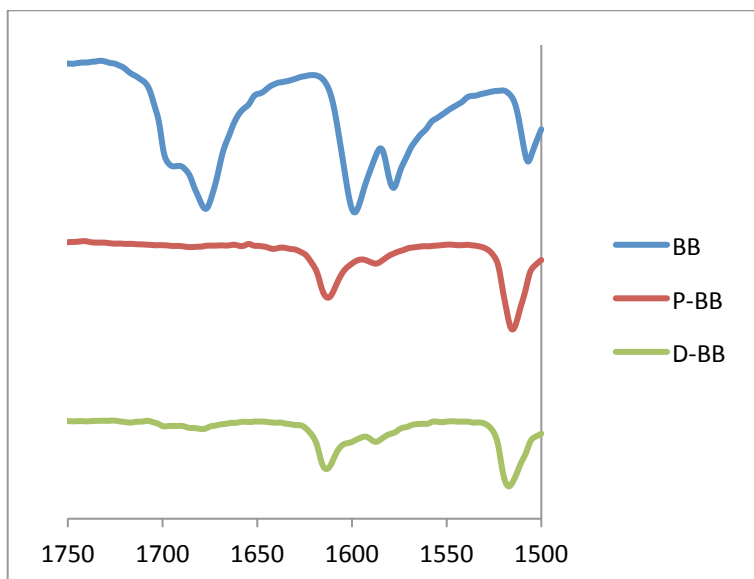


Figure S40. Comparative FTIR spectra for **BB** (monomer), **P-BB**, and **D-BB** for carbonyl area (magnified), showing no carbonyl peak in either polymer.

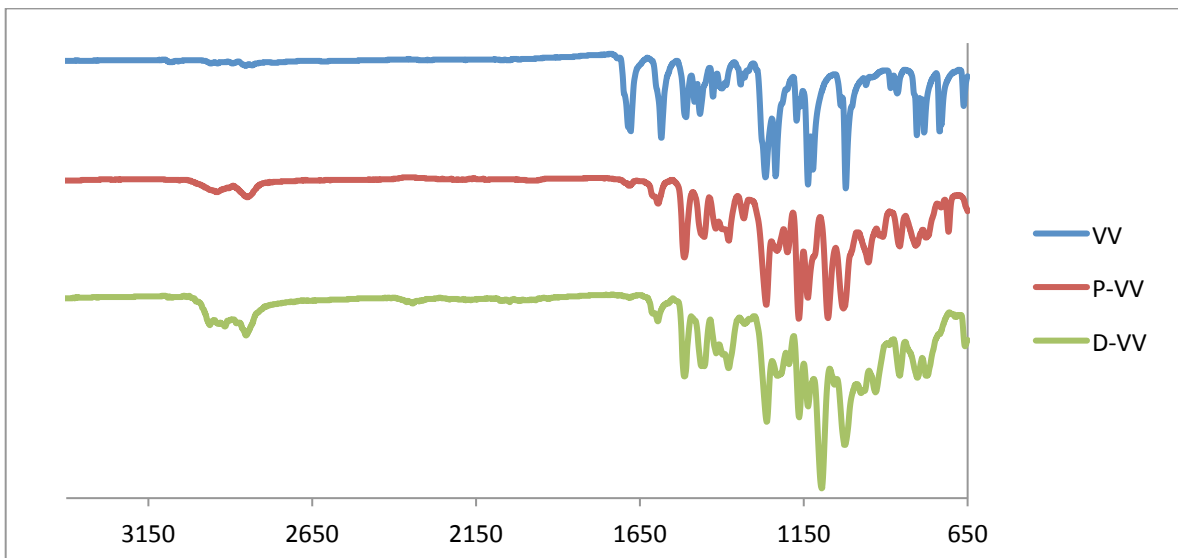


Figure S41. Comparative FTIR spectra for **VV** (monomer), **P-VV**, and **D-VV**.

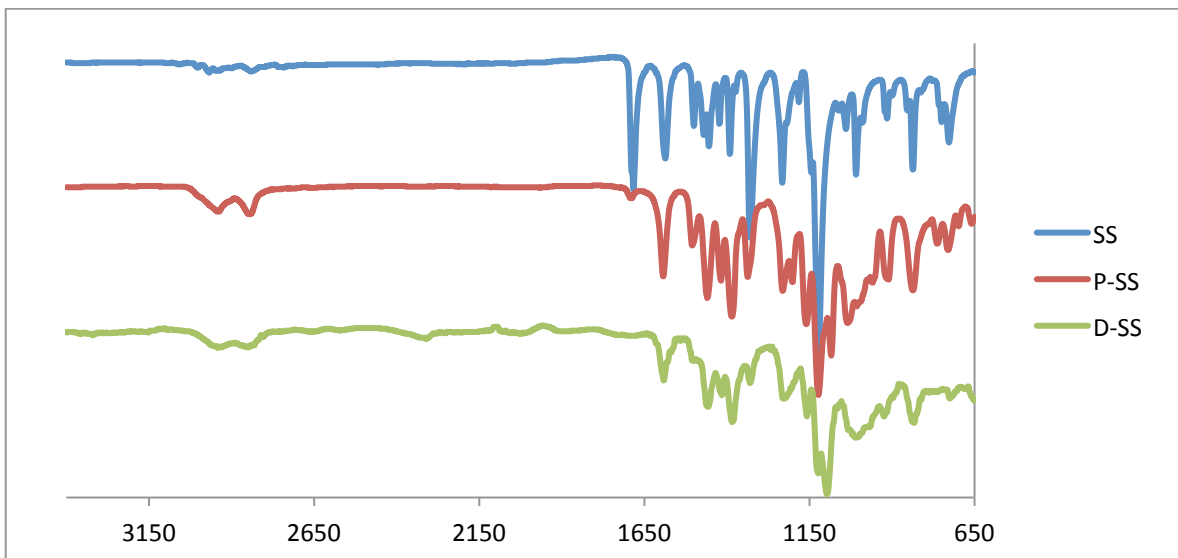


Figure S42. Comparative FTIR spectra for **SS** (monomer), **P-SS**, and **D-SS**.

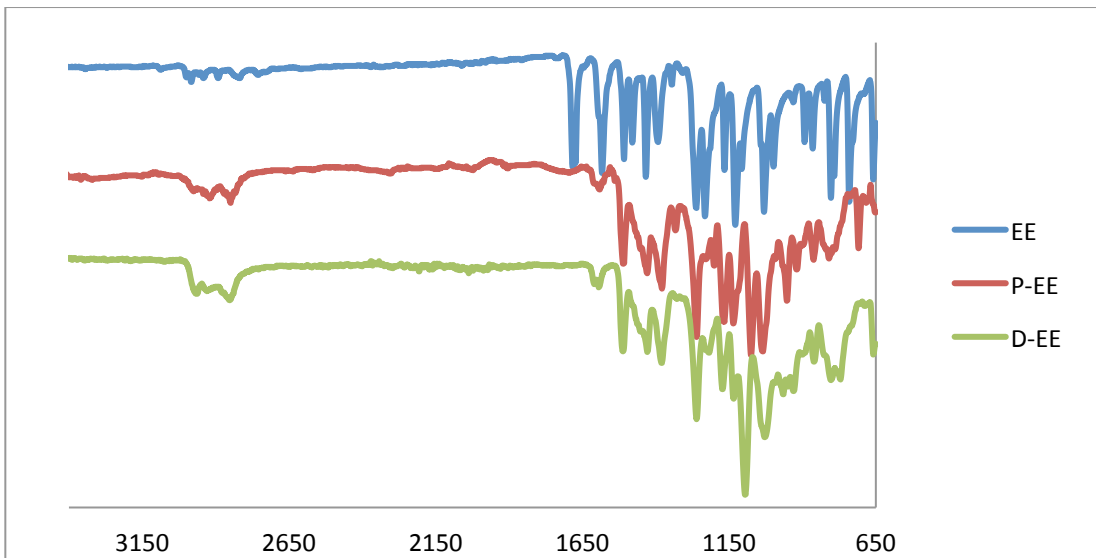


Figure S43. Comparative FTIR spectra for **EE** (monomer), **P-EE**, and **D-EE**.

Degradation Studies via Dynamic Light Scattering (DLS)

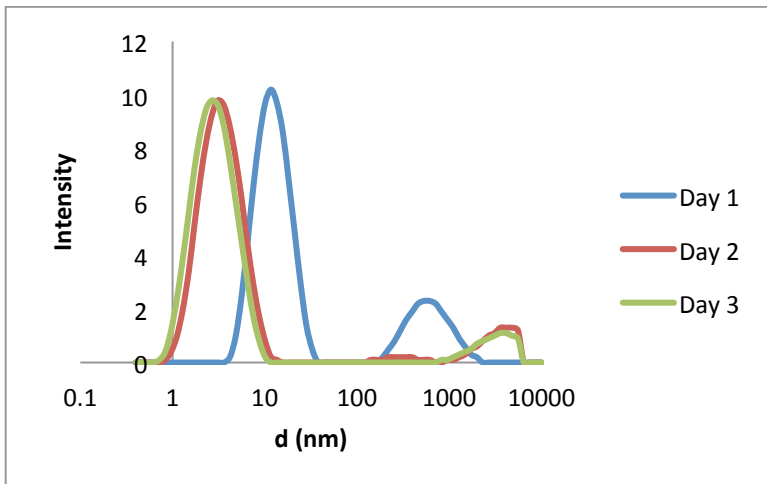


Figure S44. Degradation studies of P-VV / DMSO solution with 0.5% aqueous concentrated HCl.

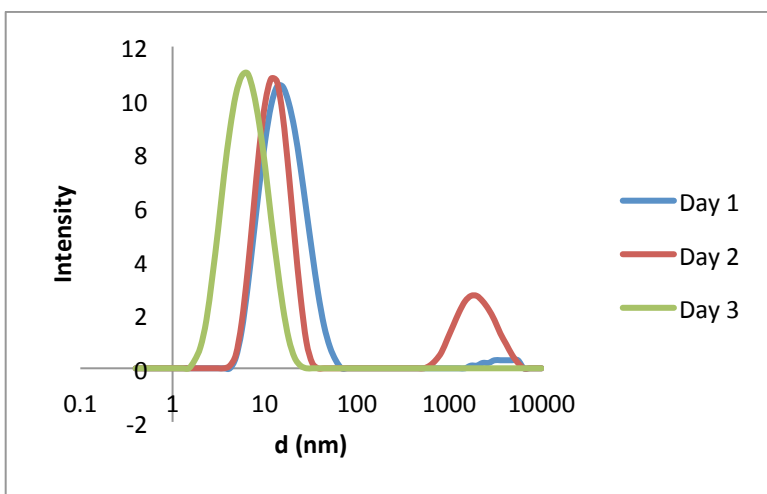


Figure S45. Degradation studies of P-VV / DMSO solution with 0.5% 2M aqueous HCl.

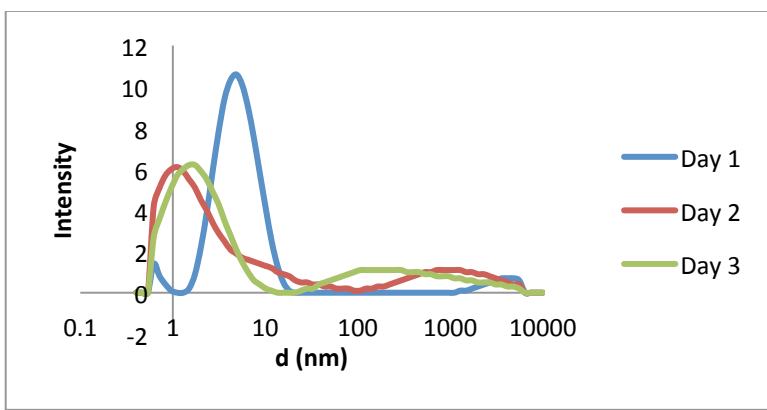


Figure S46. Degradation studies of D-VV / DMSO solution with 0.5% aqueous concentrated HCl.

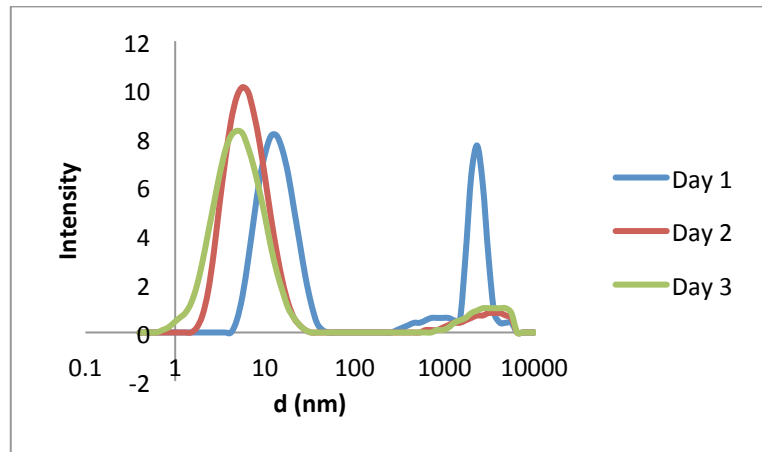


Figure S47. Degradation studies of **D-VV** / DMSO solution with 0.5% 2M aqueous HCl.